One Molecule Two Goals: A Selective P-glycoprotein Inhibitor Increases Drug Transport Across Gastro-Intestinal Barrier and Recovers Doxorubicin Toxicity in Multidrug Resistant Cancer Cells.

Marialessandra Contino,[§] Stefano Guglielmo,[,‖] Chiara Riganti,[*,§] Giulia Antonello,[§] Maria G. Perrone,[§] Roberta Giampietro,[§] Barbara Rolando,[‖] Roberta Fruttero,[‖] and Nicola A. Colabufo.[§,⊥]*

[§]Dipartimento di Farmacia-Scienze del Farmaco, Università degli Studi di Bari ALDO MORO, via Orabona 4, 70125, Bari Italy

[‖]Dipartimento di Scienza e Tecnologia del Farmaco, Università degli Studi di Torino, Via P. Giuria 9, 10125 Torino, Italy

[§]Dipartimento di Oncologia, Università degli Studi di Torino, via Santena 5/bis, 10126, Torino, Italy

[⊥]Biofordrug s.r.l., Spin-off dell'Università degli Studi di Bari ALDO MORO, Via Orabona 4, 70125 Bari, Italy

KEYWORDS Gastro-intestinal barrier; bioavailability; oral administration; multi-drug resistance; P-glycoprotein; drug design.

ABSTRACT In the present study a series of tetrahydroisoquinoline derivatives were synthesized and evaluated for their activity towards three ABC transporters, P-gp, MRP1 and BCRP. The compounds proved to be selective against P-gp. One of them, **8b**, displayed activity in the nanomolar range (EC_{50} = 94 nM). Thus, compound **8b** was tested for its ability to restore the cytotoxic activity of a well-known anti-cancer agent and P-gp substrate, doxorubicin, as first proof of concept . Moreover, compound **8b** was also tested in an in vitro model of competent gastro-intestinal (GI) barrier (Caco-2 cells) for its ability to inhibit P-gp, present on luminal side, and increase the apical-to-basolateral transport of several structurally uncorrelated drugs, belonging to different therapeutic areas but actively excreted by P-gp. Notably the transport of the drugs across the GI barrier was increased by a concentration of **8b** devoid of toxicity and of perturbing effects on barrier function. An in vitro simulated digestion process was set up: interestingly the effect **8b** on the transport of digoxin was preserved also after the simulated digestion process. This result may suggest **8b** as a safe and effective P-gp inhibitor that can increase the bioavailability of a wide-spectrum of drugs administered *per os*, improving their transport across the GI barrier.

INTRODUCTION

Gastro-intestinal (GI) mucosa is a physiological barrier regulating the passage of nutrients, drugs and pathogens from the external environment into the systemic circulation.[1] Mucins and glycoproteins constitute a protective line on the luminal side of the epithelial cells, that mostly contribute to the barrier properties of GI tract.[1]

The network of tight junctions (TJs), together with adherens junctions (AJs) and desmosomes in the peri-junctional plasma-membrane of epithelial cells, is one of the main factors contributing to the epithelial integrity and limiting the paracellular diffusion of substrates.[2] TJs are composed by integral proteins of claudin, occludin and zonula occludens (ZO) families, and junctional adhesion molecules (JAMs)[3]: the presence of all these components indicate that the physiological functions of GI barrier are maintained. Indeed, TJs are qualitatively and quantitatively altered in inflammatory bowel diseases and severe colitis, where the permeability to substrates, toxins and gut microbes dramatically increase.[2,3]

A second system limiting the transcellular diffusion of substrates is represented by the apical transporters, belonging to the ATP Binding Cassette (ABC) transporters and organic anion transporter proteins (OATPs). Both families can efflux substrates back into the intestinal lumen and therefore regulate the transport of nutrients to the systemic circulation. Moreover, they are well known modulators of the absorption, distribution and excretion (ADE) process of orally assumed drugs.[4,5] P-glycoprotein (P-gp) [4,5] and multidrug resistance related proteins, namely MRP1 and MRP2, [5,6] are the ABC transporters mostly expressed in GI epithelium. P-gp levels increase from duodenum to colon and physiologically act as a detoxifier and a regulator of the homeostasis established between mucosa and gut microbioma.[7] A defective P-gp predisposes to the onset of colitis and inflammatory bowel diseases,[8] while its overexpression strongly limits drug disposition, because P-gp recognizes a broad spectrum of substrates, including anticancer,

anti-hypertensive, anti-convulsant, anti-arhythmics, anti-depressant, anti-retroviral, anti-microbial agents commonly prescribed.[5] For this reason, a strategy commonly employed to improve the bioavailability of drugs, allowing them to exert their efficacious activity, has been their co-administration with potent P-gp ligands. This approach has been used in cancer therapy to overcome multidrug resistance (MDR), i.e. the simultaneous resistance to multiple chemotherapeutic drugs because of their efflux via P-gp [9–11] and may be therefore an effective strategy in oncological settings. It has been several years since the authors started dealing with the development of highly potent and selective P-gp ligands, with the aim to hit the undesirable effect due to P-gp mediated efflux of unrelated chemical entities acting as drugs.[12,13,22–28,14–21]

Starting from our lead compound **MC70**, bearing a tetrahydroisoquinoline scaffold, displaying high potency vs P-gp[14], we proceeded in the design and biological evaluation of several series of P-gp compounds identifying compound **1** that emerged as a P-gp ligand able to overcome MDR in cancer stem cells (Chart 1).[25]

Chart 1.

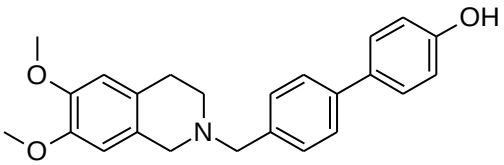

MC70

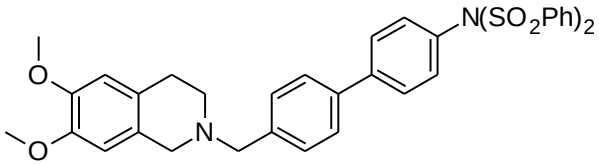

1

Starting from this compound, in the present study we performed a structural modulation on the sulfonamide moiety, according to three different approaches: the first sub-series is made up of arylsulfonamides bearing substituents with different stereoelectronic properties (compounds **5b-g**). The second was obtained retaining the (*N*-sulfonyl)sulfonamide substructure of **1**

"duplicating" the arylsulfonamide moieties of the first sub-series (compounds **8b-f**), except for the bulkier naphtalensulfonamide derivative **5g**. In the last approach, starting from the benzenesulfonamide substructure, a series of *N*-alkyl and *N*-arylmethyl derivatives was obtained (compounds **14a-g**), characterized by an ample modulation of steric properties (Scheme 1).

The compounds were studied for their mechanism of interaction, potency and selectivity towards P-gp and its sister proteins MRP1 and breast cancer resistance protein (BCRP), also involved in MDR and in the efflux of several drugs from gut. Among them, compound **8b**, belonging to the second sub-series and bearing 4-methoxybenzenesulfonyl rings, displayed activity towards P-gp in the nanomolar range, even though it was less potent than the parent compound.

Compound **8b** was then subjected to more detailed studies: it was tested in co-administration with the anticancer agent Doxorubicin, a well-known P-gp substrate, in MDCK cells constitutively overexpressing P-gp, and in an in vitro model of Caco-2 GI barrier. The results of this characterization allow to candidate compound **8b** as an active compound able to exert a double action: 1) restore the sensitivity of resistant tumours to antineoplastic drugs substrate of P-gp and 2) improve the bioavailability of several structurally unrelated and orally administered drugs, all P-gp substrates.

EXPERIMENTAL SECTION

CHEMISTRY

General synthetic methods. ^{1}H and ^{13}C-NMR spectra were recorded on a Jeol 600 at 600 and 150 MHz respectively. Chemical shifts (δ) are given in parts per million (ppm). The following abbreviations are used to designate the multiplicities: s = singlet, d = doublet, dd = doublet of

doublets, t = triplet, q = quartet, quin = quintuplet, m = multiplet. Low resolution mass spectra were recorded on a Micromass Quattro micro^{TM} API (Waters Corporation, Milford, MA, USA) with electrospray ionization (ESI) or atmospheric pressure ionization (API). Melting points (mp) were determined with a capillary apparatus (Büchi 540). Flash column chromatography was performed on silica gel (Merck Kieselgel 60, 230-400 mesh ASTM). The progress of the reactions was followed by thin layer chromatography (TLC) on 5×20 cm plates with a layer thickness of 0.2 mm. The purity of target compounds was assessed by RP-HPLC. Analyses were performed on a HP1100 chromatograph system (Agilent Technologies, Palo Alto, CA, USA) equipped with a quaternary pump (G1311A), a membrane degasser (G1379A), a diode-array detector (DAD) (G1315B) integrated in the HP1100 system. Data analysis were processed by HP ChemStation system (Agilent Technologies). The analytical column was a LiChrospher® 100 C18-e (250×4.6mm, 5µm) (Merck KGaA, 64271 Darmstadt, Germany) eluted with CH_3CN/H_2O 0.1% TFA in a ratio depending on the characteristics of the compound. All compounds were dissolved in the mobile phase at a concentration of about 0.1 mg/ml and injected through a 20 µL loop. The DAD acquired the UV spectra in the range from 190 to 360 nm, and the HPLC chromatogram was recorded at 210, 226 and 254 nm (with 360 nm as reference wavelength)The purity of the test samples was evaluated as a percentage ratio between the areas of the main peak and of possible impurities at the three wavelengths and also using DAD purity analysis of the chromatographic peak. The purity of all target compounds resulted ≥ 95%. Compound **2** was prepared according to a reported procedure.[25]

General procedure for the synthesis of compounds 3a-g. Compound **2** (5 mmol), the appropriate sulfonyl chloride (1.2 eq.) and pyridine (1.5 eq.) were dissolved in CH_2Cl_2. The solution was stirred at room temperature for 6 hours. The mixture was then washed with HCl

1M, saturated solution of $NaHCO_3$, brine, dried over Na_2SO_4, filtered and concentrated under reduced pressure. The crude product was purified through flash chromatography on silica gel.

N-[4'-(hydroxymethyl)-[1,1'-biphenyl]-4-yl]benzenesulfonamide (3a). Eluent: petroleum ether / acetone 70 / 30. White solid. Yield: 68%. Mp (iPrOH): 112.5 – 113.2 °C. ESI^- MS: 338 ($M-H^-$). ^{1}H-NMR (D^6-DMSO): δ 10.44 (s, 1H); 7.6 (d, *J* = 6.9 Hz, 2H); 7.56 (m, 7H); 7.35 (d, *J* = 8.3 Hz, 2H); 7.19 (m, 2H); 5.16 (br. s. 1H); 4.51 (s, 2H). ^{13}C-NMR (D^6-DMSO): δ 141.6, 139.6, 137.6, 136.9, 135.7, 133.0, 129.4, 127.2, 127.0, 126.7, 126.0, 120.3, 62.6.

N-[4'-(hydroxymethyl)-[1,1'-biphenyl]-4-yl]-4-methoxybenzene-1-sulfonamide (3b). Eluent: petroleum ether / acetone 70 / 30. White solid. Yield: 56%. Mp (iPrOH): 130 – 130.7 °C. ESI^- MS: 368 ($M-H^-$). ^{1}H-NMR (D^6-DMSO): δ 10.28 (br. s, 1H); 7.73 (d, *J* = 8.6 Hz, 2H); 7.53 (d, *J* = 8.6 Hz, 4H); 7.35 (d, *J* = 7.9 Hz, 2H); 7.17 (d, 2H, *J* = 8.6 Hz, 2H); 7.06 (d, *J* = 9.0 Hz, 2H); 5.20 (br. s., 1H); 4.51 (br. s, 2H); 3.78 (s, 3H). ^{13}C-NMR (D^6-DMSO): δ 141.6, 139.6, 137.6, 136.9, 135.7, 133.0, 129.4, 127.2, 127.0, 126.7, 126.0, 120.3, 62.6, 55.6.

4-fluoro-N-[4'-(hydroxymethyl)-[1,1'-biphenyl]-4-yl]benzene-1-sulfonamide (3c). Eluent: petroleum ether / acetone 80 / 20. White solid. Yield: 72%. Mp (CH_3OH): 132.3 – 133 °C. ESI^- MS: 356 ($M-H^-$). ^{1}H-NMR ($CDCl_3$): δ 7.82 (m, 2H); 7.49 (d, *J* = 8.3 Hz, 2H); 7.45 (m, 2H); 7.40 (d, *J* = 8.3 Hz, 2H); 7.12 (m, 4H); 4.73 (s, 2H). ^{13}C-NMR ($CDCl_3$): δ 165.4 (d, *J* = 255 Hz), 140.1, 138.2, 135.5, 135.2, 135.2, 130.1 (d, *J* = 10.5 Hz), 128.0, 127.7, 127.1, 122.3, 116.5 (d, *J* = 21 Hz), 65.1.

4-chloro-N-[4'-(hydroxymethyl)-[1,1'-biphenyl]-4-yl]benzene-1-sulfonamide (3d). Eluent: petroleum ether / CH_2Cl_2 / acetone 35 / 60 / 5. White solid. Yield: 60%. Mp (iPrOH): 173.8 - 175

°C. ESI$^-$ MS: 372 / 374 (M-H$^-$). ^{1}H-NMR (D^6-DMSO): δ 10.49 (s, 1H); 7.78 (d, *J* = 9.0 Hz, 2H); 7.65 (d, *J* = 9.0 Hz 2H); 7.55 (m, 4H); 7.35 (d, *J* = 8.6 Hz, 2H); 7.17 (d, *J* = 9 Hz, 2H); 4.51 (s, 3H, two overlapping signals). ^{13}C-NMR (D^6-DMSO): δ 142.2, 138.9, 138.4, 138.1, 137.1, 136.5, 130.0, 129.2, 127.8, 127.5, 126.5, 121.2, 63.1.

4-bromo-N-[4'-(hydroxymethyl)-[1,1'-biphenyl]-4-yl]benzene-1-sulfonamide (3e). Eluent: petroleum ether / CH_2Cl_2 / acetone 35 / 60 / 5. White solid. Yield: 62%. Mp (iPrOH): 249.6 – 250.4 °C. ESI$^-$ MS: 416 / 418 (M-H$^-$). ^{1}H-NMR (D^6-DMSO): δ 10.51 (s, 1H); 7.78 (d, *J* = 8.6 Hz, 2H); 7.71 (d, *J* = 9 Hz, 2H); 7.55 (m, 4H); 7.35 (d, *J* = 8.3 Hz, 2H); 7.17 (d, *J* = 8.6 Hz, 2H); 5.22 (t, *J* = 5.7 Hz, 1H); 4.51 (d, *J* = 5.5 Hz, 2H). ^{13}C-NMR (D^6-DMSO): δ 142.2, 139.3, 138.1, 137.1, 136.5, 133.0, 129.2, 127.8, 127.5, 127.4, 126.5, 121.1, 63.1.

N-[4'-(hydroxymethyl)-[1,1'-biphenyl]-4-yl]-4-nitrobenzene-1-sulfonamide (3f). Eluent: petroleum ether / acetone 70 / 30. Pale yellow solid. Yield: 55%. Mp (EtOH): 183.3 – 184.0 °C. ESI$^-$ MS: 383 (M-H$^-$). ^{1}H-NMR (D^6-DMSO): δ 10.52 (br. s., 1H); 8.38 (d, *J* = 9.0 Hz, 2H); 8.04 (d, *J* = 9.0 Hz, 2H); 7.56 (d, *J* = 8.6 Hz, 2H); 7.53 (d, *J* = 7.9 Hz, 2H); 7.35 (d, *J* = 8.3 Hz, 2H); 7.19 (d, *J* = 8.6 Hz, 2H); 5.20 (br. s., 1H); 4.51 (s, 2H). ^{13}C-NMR (D^6-DMSO): δ 150.4, 145.5, 142.2, 138.0, 136.9, 136.7, 128.8, 127.9, 127.5, 126.6, 125.3, 121.5, 63.1.

N-[4'-(hydroxymethyl)-[1,1'-biphenyl]-4-yl]naphthalene-1-sulfonamide (3g). Eluent: petroleum ether / acetone 80 / 20. White solid. Yield: 49%. Mp (MeOH): 192.1 – 193.6 °C. ESI$^-$ MS: 388 (M-H$^-$). ^{1}H-NMR (D^6-DMSO): δ 10.84 (s, 1H); 8.77 (d, *J* = 8.6 Hz, 1H); 8.27 (d, *J* = 7.2 Hz, 1H); 8.21 (d, *J* = 8.3 Hz, 1H); 8.07 (d, *J* = 8.3 Hz, 1H); 7.76 (t, *J* = 7.7 Hz, 1H); 7.65 (m, 2H); 7.46 (t, *J* = 7.2 Hz, 4H); 7.31 (d, *J* = 8.3 Hz, 2H); 7.12 (d, *J* = 8.6 Hz, 2H); 5.19 (t, *J* = 5.7

Hz, 1H); 4.49 (d, *J* = 5.9 Hz, 2H). ^{13}C-NMR (D^6-DMSO): δ 142.0, 138.2, 137.3, 135.7, 135.0, 134.9, 134.3, 130.5, 129.7, 128.7, 128.0, 127.7, 127.5, 126.4, 125.5, 125.0, 124.8, 119.7, 63.1.

General procedure for the synthesis of compounds 5b-g. Compounds **3b-g** (1 mmol) were dissolved in 10 mL of THF; the solution was cooled in an ice bath and pyridine (5 eq.) and SO_2Cl_2 (5 eq.) were added; the mixture was allowed to warm to room temperature and was stirred for 1 hour. After that rime it was diluted with water and extracted with CH_2Cl_2; the organic phase was washed with HCl 1M, saturated solution of $NaHCO_3$, brine, dried over Na_2SO_4, filtered and concentrated under reduced pressure. The crude product was dissolved in 20 mL of CH_3CN and 6,7-dimethoxy-1,2,3,4-tetrahydroisoquinoline hydrochloride (1.3 eq.) and 1,5-diazabicyclo(5.4.0)undec-7-ene (2.5 eq.) were added. The mixture was stirred at 70 °C for 8 hours. The mixture was concentrated under reduced pressure; the residue was taken up with CH_2Cl_2, washed with water, brine, dried over Na_2SO_4, filtered and concentrated under reduced pressure. The crude product was purified through flash chromatography o silica gel.

N-{4'-[(6,7-dimethoxy-1,2,3,4-tetrahydroisoquinolin-2-yl)methyl]-[1,1'-biphenyl]-4-yl}-4-methoxybenzene-1-sulfonamide (5b). Eluent: CH_2Cl_2 / acetone 95 / 5. White solid. Yield: 87%. Mp (iPrOH): 230.2 - 231.8 °C. ESI$^+$ MS: 545 (M+H$^+$). ^{1}H-NMR (D^6-DMSO): δ 10.29 (br. s., 1H); 7.74 (d, *J* = 9.0 Hz, 2H); 7.54 (d, *J* = 8.3 Hz, 4H); 7.37 (d, *J* = 8.3 Hz, 2H); 7.18 (d, *J* = 8.6 Hz, 2H); 7.06 (d, *J* = 9.0 Hz, 2H); 6.64 (s, 1H); 6.56 (s, 1H); 3.77 (s, 3H); 3.68 (s, 3H); 3.62 (s, 3H); 3.42 (s, 2H); 3.36 (br. s., 2H); 2.71 (t, *J* = 5.3 Hz, 2H); 2.64 (t, *J* = 5.7 Hz, 2H). ^{13}C-NMR (D^6-DMSO): δ 162.4, 147.1, 146.9, 138.0, 137.5, 137.3, 135.3, 131.2, 129.3, 128.9, 127.2, 126.5, 126.1, 125.8, 120.1, 114.4, 111.8, 109.9, 61.6, 55.6, 55.4, 55.4, 55.0, 50.5, 28.3.

N-{4'-[(6,7-dimethoxy-1,2,3,4-tetrahydroisoquinolin-2-yl)methyl]-[1,1'-biphenyl]-4-yl}-4-fluorobenzene-1-sulfonamide (5c). Eluent: CH_2Cl_2 / acetone 95 / 5. White solid. Yield: 52%. Mp (iPrOH): 192 - 195 °C (dec.). ESI^+ MS: 533 ($M+H^+$). ^{1}H-NMR ($CDCl_3$): δ 7.79 (dd, *J* = 8.8 Hz, 2H); 7.46 (m, 7H); 7.10 (m, 4H); 6.60 (s, 1H); 6.49 (s, 1H); 3.83 (s, 3H); 3.80 (s, 3H); 3.71 (s, 2H); 3.58 (s, 2H); 2.83 (t, *J* = 5.9 Hz, 2H); 2.76 (t, *J* = 5.9 Hz, 2H). ^{13}C-NMR ($CDCl_3$): δ 165.3 (d, *J* = 253.5 Hz), 147.6, 147.3, 138.8, 138.3, 137.7, 135.4, 135.2, 130.1 (d, *J* = 10.5 Hz), 129.8, 128.0, 126.8, 126.7, 126.2, 122.4, 116.4 (d, *J* = 22.5 Hz), 111.5, 109.6, 62.4, 56.0 (two overlapping signals); 55.8, 50.9, 28.8.

4-chloro-N-{4'-[(6,7-dimethoxy-1,2,3,4-tetrahydroisoquinolin-2-yl)methyl]-[1,1'-biphenyl]-4-yl}benzene-1-sulfonamide (5d). Eluent: CH_2Cl_2 / acetone 95 / 5. White solid. Yield: 31%. Mp (iPrOH): 199.0 - 201.4 °C. ESI^+ MS: 549 / 551 ($M+H^+$). ^{1}H-NMR ($CDCl_3$): δ 7.70 (m, 2H); 7.47 (m, 5H); 7.44 (m, 1H); 7.43 (s, 1H); 7.40 (m, 2H); 7.11 (m, 2H); 6.60 (s, 1H); 6.49 (s, 1H); 3.84 (s, 3H); 3.80 (s, 3H); 3.71 (s, 2H); 3.58 (s, 2H); 2.83 (t, *J* = 5.7 Hz, 2H); 2.76 (t, *J* = 5.9 Hz, 2H). ^{13}C-NMR ($CDCl_3$): δ 147.6, 147.3, 139.7, 138.8, 138.5, 137.8, 137.7, 135.3, 129.8, 129.5, 128.8, 128.0, 126.8, 126.7, 126.2, 122.5, 111.5, 109.6, 62.5, 56.0 (two overlapping signals), 55.8, 50.9, 28.8.

4-bromo-N-{4'-[(6,7-dimethoxy-1,2,3,4-tetrahydroisoquinolin-2-yl)methyl]-[1,1'-biphenyl]-4-yl}benzene-1-sulfonamide (5e). Eluent: CH_2Cl_2 / acetone 95 / 5. White solid. Yield: 47%. Mp (EtOH): 133.0 - 132.3 °C. ESI^+ MS: 593 / 595 ($M+H^+$). ^{1}H-NMR ($CDCl_3$): δ 7.62 (m, 2H); 7.57 (m, 2H); 7.48 (m, 4H); 7.44 (m, 3H); 7.12 (d, *J* = 8.6 Hz, 2H); 6.60 (s, 1H); 6.48 (s, 1H); 3.84 (s, 3H); 3.80 (s, 3H); 3.72 (s, 2H); 3.58 (s, 2H); 2.84 (m, 2H); 2.77 (d, *J* = 5.2 Hz, 2H). ^{13}C-NMR

($CDCl_3$): δ 147.6, 147.3, 138.9, 138.8, 138.6, 138.3, 138.2, 135.2, 132.5, 129.8, 128.9, 128.3, 128.1, 127.9, 126.9, 122.6, 111.5, 109.5, 56.0 (two overlapping signals), 55.80, 55.76, 50.9, 29.4.

N-{4'-[(6,7-dimethoxy-1,2,3,4-tetrahydroisoquinolin-2-yl)methyl]-[1,1'-biphenyl]-4-yl}-4-nitrobenzene-1-sulfonamide (5f). Eluent: CH_2Cl_2 / acetone 93 / 7. Pale yellow solid. Yield: 81%. Mp (MeOH): 175.4 – 178.0 °C (dec.). ESI^+ MS: 560 ($M+H^+$). ^{1}H-NMR ($CDCl_3$): δ 8.24 (m, 2H); 7.87 (m, 2H); 7.44 (m, 7H); 7.09 (m, 2H); 6.59 (s, 1H); 6.50 (s, 1H); 3.84 (s, 3H); 3.80 (s, 3H); 3.71 (s, 2H); 3.60 (s, 2H); 2.83 (t, J = 5.7 Hz, 2H); 2.78 (t, J = 5.7 Hz, 2H). ^{13}C-NMR ($CDCl_3$): δ 150.2, 147.7, 147.4, 145.0, 139.0, 138.6, 137.6, 134.8, 129.9, 128.5, 128.1, 126.8, 126.6, 126.2, 124.3, 122.9, 111.5, 109.6, 62.4, 56.0 (two overlapping signals), 55.8, 50.8, 28.6.

N-{4'-[(6,7-dimethoxy-1,2,3,4-tetrahydroisoquinolin-2-yl)methyl]-[1,1'-biphenyl]-4-yl}naphthalene-1-sulfonamide (5g). Eluent: CH_2Cl_2 / acetone 95 / 5. White solid. Yield: 76%. Mp (MeOH): 82.0 – 82.7 °C. ESI^+ MS: 565 ($M+H^+$). ^{1}H-NMR ($CDCl_3$): δ 8.70 (d, J = 8.6 Hz, 1H); 8.21 (d, J = 8.6 Hz, 1H); 8.04 (d, J = 8.3 Hz, 1H); 7.94 (d, J = 8.3 Hz, 1H); 7.70 (m, 1H); 7.61 (m, 1H); 7.46 (m, 1H); 7.41 (m, 4H); 7.37 (m, 2H); 6.98 (m, 2H); 6.83 (br. s., 1H); 6.59 (s, 1H); 6.47 (s, 1H); 3.83 (s, 3H); 3.79 (s, 3H); 3.68 (s, 2H); 3.54 (s, 2H,); 2.82 (t, 2H, J = 5.7 Hz, 2H); 2.73 (t, J = 5.9 Hz, 2H). ^{13}C-NMR ($CDCl_3$): δ 147.6, 147.2, 141.0, 137.8, 136.4, 135.3, 134.8, 134.3, 130.5, 129.6, 129.4, 128.7, 128.2, 127.8, 127.0, 126.8, 126.2, 124.23, 124.19, 122.3, 120.4, 111.5, 109.5, 102.4, 62.5, 55.99, 55.97, 55.8, 50.9, 28.8.

General procedure for the synthesis of compounds 6b-f. Compounds **3b-f** (5 mmol) were dissolved in 15 mL of CH_3CN; Et_3N (2 eq.) and arylsulfonyl chloride (1.7 eq.) were added and the mixture was stirred at 70 °C for 8 hours. After that time the solvent was distilled under reduced pressure and the residue was taken up with CH_2Cl_2; the organic phase was washed with

water, HCl 1M, saturated solution of $NaHCO_3$, brine, dried over Na_2SO_4, filtered and concentrated under reduced pressure. The crude product was purified through flash chromatography on silica gel. Intermediate **6f** could not be isolated: after the reaction the chloride derivative **7f** was isolated and characterized.

N-[4'-(hydroxymethyl)-[1,1'-biphenyl]-4-yl]-4-methoxy-N-(4-methoxybenzenesulfonyl)benzene-1-sulfonamide (6b). Eluent: petroleum ether / acetone 50 / 50. White solid. Yield: 47%. Mp (iPrOH): 232.3 - 232.6 °C. ESI^+ MS: 562 ($M+Na^+$). ^{1}H-NMR (D^6-DMSO): δ 7.78 (m, 4H); 7.73 (d, *J* = 8.6 Hz, 2H); 7.67 (d, *J* = 7.9 Hz, 2H); 7.43 (d, *J* = 8.3 Hz, 2H); 7.20 (m, 4H); 7.06 (m, 2H); 5.27 (t, *J* = 5.9 Hz, 1H); 4.56 (d, *J* = 5.9 Hz, 2H); 3.90 (s, 6H two overlapping signals). ^{13}C-NMR (D^6-DMSO): δ 163.8, 142.7, 141.8, 136.9, 132.8, 131.7, 130.5, 130.0, 127.4, 127.1, 126.6, 114.7, 62.5, 56.0.

4-fluoro-N-(4-fluorobenzenesulfonyl)-N-[4'-(hydroxymethyl)-[1,1'-biphenyl]-4-yl]benzene-1-sulfonamide (6c). Eluent: petroleum ether / acetone 80 / 20. White solid. Yield: 47%. Mp (iPrOH): 205.7 - 206.6 °C. API^+ MS: 516 ($M+H^+$). ^{1}H-NMR (D^6-DMSO): δ 7.95 (m, 4H); 7.76 (d, *J* = 8.6 Hz, 2H); 7.68 (d, 2H, *J* = 8.3 Hz, 2H); 7.57 (m, 4H); 7.44 (d, *J* = 8.6 Hz, 2H); 7.12 (d, *J* = 8.6 Hz, 2H); 5.28 (t, J=5.9 Hz, 1H); 4.56 (d, *J* = 5.9 Hz, 2H). ^{13}C-NMR (D^6-DMSO): δ 166.0 (d, *J* = 253.5 Hz), 143.3, 142.7, 137.3, 135.2, 132.7, 132.3, 132.0 (d, *J* = 10.5 Hz), 128.2, 127.6, 127.2, 117.6 (d, *J* = 24 Hz), 63.05.

4-chloro-N-(4-chlorobenzenesulfonyl)-N-[4'-(hydroxymethyl)-[1,1'-biphenyl]-4-yl]benzene-1-sulfonamide (6d). Eluent: petroleum ether / acetone 85 / 15. White solid. Yield: 45%. Mp (iPrOH): 179.0-180.2 °C. ESI^+ MS: 570 / 572 / 574 ($M+Na^+$). ^{1}H-NMR (D^6-DMSO): δ 7.90 (m, 4H); 7.80 (m, 4H); 7.77 (d, *J* = 9.0 Hz, 2H); 7.68 (m, 2H); 7.44 (d, *J* = 8.6 Hz, 2H); 7.15 (d, *J* =

8.6 Hz, 2H); 4.83 (br. s., 1H); 4.56 (s, 2H). ^{13}C-NMR (D^6-DMSO): δ 143.3, 142.8, 140.5, 137.7, 132.6, 132.3, 130.6, 130.4, 130.1, 128.2, 127.6, 127.2, 63.1.

4-bromo-N-(4-bromobenzenesulfonyl)-N-[4'-(hydroxymethyl)-[1,1'-biphenyl]-4-yl]benzene-1-sulfonamide (6e). Eluent: petroleum ether / acetone 80 / 20. White solid. Yield: 30%. Mp (MeOH): 214.0 – 217.5 °C (dec.). ESI$^+$ MS: 658 / 660 / 662 (M+Na$^+$). ^{1}H-NMR ($CDCl_3$): δ 7.83 (m, 4H); 7.72 (m, 4H); 7.59 (m, 4H); 7.47 (d, *J* = 8.3 Hz, 2H); 7.09 (m, 2H); 4.77 (d, *J* = 4.5 Hz, 2H); 1.75 (t, *J* = 5.0 Hz, 1H). ^{13}C-NMR ($CDCl_3$): δ 143.1, 140.8, 138.7, 138.2, 132.7, 132.4, 131.6, 130.0, 129.5, 129.2, 128.0, 127.4, 64.9.

N-[4'-(chloromethyl)-[1,1'-biphenyl]-4-yl]-4-nitro-N-(4-nitrobenzenesulfonyl)benzene-1-sulfonamide (7f). Eluent: petroleum ether / CH_2Cl_2 30 / 70. White solid. Yield: 46%. Mp (iPr_2O): 275.2 – 278.5 °C (dec.). ESI$^+$ MS: 610 / 612 (M+Na$^+$). ^{1}H-NMR (D^6-DMSO): δ 8.53 (m, 4H); 8.16 (m, 4H); 7.81 (m, 2H); 7.75 (d, *J* = 8.3 Hz, 2H); 7.57 (d, *J* = 8.3 Hz, 2H); 7.24 (m, 2H); 4.83 (s, 2H). ^{13}C-NMR (D^6-DMSO): δ 151.5, 143.6, 142.6, 138.8, 138.4, 132.4, 130.5, 130.2, 129.9, 128.7, 127.8, 125.6, 46.3.

General procedure for the synthesis of target compounds 8b-f. The target compounds were obtained through the same synthetic path used for compounds **5b-g**.

N-{4'-[(6,7-dimethoxy-1,2,3,4-tetrahydroisoquinolin-2-yl)methyl]-[1,1'-biphenyl]-4-yl}-4-methoxy-N-(4-methoxybenzenesulfonyl)benzene-1-sulfonamide (8b). Eluent: CH_2Cl_2 / ethyl acetate 90 / 10. White solid. Yield: 78%. Mp (EtOH): 106.7 - 107.9 °C. ESI$^+$ MS: 715 (M+H$^+$). ^{1}H-NMR ($CDCl_3$): δ 7.90 (m, 4H); 7.57 (m, 4H); 7.48 (d, *J* = 8.3 Hz, 2H); 7.09 (m, 2H); 7.00 (m, 4H); 6.61 (s, 1H); 6.50 (s, 1H); 3.90 (s, 6H); 3.84 (s, 3H); 3.81 (s, 3H); 3.72 (s, 2H); 3.58 (s,

2H); 2.85 (t, *J* = 5.9 Hz, 2H); 2.77 (t, *J* = 5.9 Hz, 2H). ^{13}C-NMR ($CDCl_3$): δ 171.2, 164.0, 147.6, 147.3, 142.8, 138.6, 133.5, 131.9, 131.2, 131.0, 129.7, 127.8, 127.2, 126.7, 126.3, 114.2, 111.5, 109.6, 62.5, 56.0 (two overlapping signals), 55.8 (two overlapping signals), 51.0, 28.8.

N-{4'-[(6,7-dimethoxy-1,2,3,4-tetrahydroisoquinolin-2-yl)methyl]-[1,1'-biphenyl]-4-yl}-4-fluoro-N-(4-fluorobenzenesulfonyl)benzene-1-sulfonamide (8c). Eluent: CH_2Cl_2 / acetone 95 / 5. White solid. Yield: 77%. Mp (iPrOH): 135.0 - 135.4 °C. ESI$^+$ MS: 691 (M+H$^+$). ^{1}H-NMR (D^6-DMSO): δ 7.95 (m, 4H); 7.77 (d, *J* = 8.6 Hz, 2H); 7.69 (d, 2H, *J* = 7.9 Hz, 2H); 7.57 (m, 4H); 7.48 (d, 2H, *J* = 6.9 Hz, 2H); 7.13 (d, *J* = 8.3 Hz, 2H); 6.67 (s, 1H); 6.59 (s, 1H); 3.68 (m, 8H, overlapping signals); 3.46 (br. s., 2H); 2.75 (br. s., 2H); 2.68 (br. s., 2H). ^{13}C-NMR (D^6-DMSO): δ 165.5 (d, *J* = 253.5 Hz), 147.2, 146.9, 142.1, 137.2, 134.7, 132.2, 131.8, 131.5 (d, *J* = 10.5 Hz), 129.5, 127.7, 126.8, 125.7, 117.4, 117.0 (d, *J* = 24 Hz), 111.8, 109.9, 109.5, 61.5, 55.4 (two overlapping signals), 55.1, 50.6, 28.4.

4-chloro-N-(4-chlorobenzenesulfonyl)-N-{4'-[(6,7-dimethoxy-1,2,3,4-tetrahydroisoquinolin-2-yl)methyl]-[1,1'-biphenyl]-4-yl}benzene-1-sulfonamide (8d). Eluent: petroleum ether / acetone 80 / 20. White solid. Yield: 60%. Mp (iPrOH): 220.0 – 224.5 °C (dec.). ESI$^+$ MS: 723 / 725 / 727 (M+H$^+$). ^{1}H-NMR ($CDCl_3$): δ 7.91 (m, 4H); 7.60 (d, *J* = 8.6 Hz, 2H); 7.55 (m, 6H); 7.50 (m, 2H); 7.08 (d, *J* = 8.6 Hz, 2H); 6.61 (s, 1H); 6.50 (s, 1H); 3.85 (s, 3H); 3.81 (s, 3H); 3.74 (s, 2H); 3.59 (s, 2H); 2.85 (s, 2H); 2.78 (s, 2H). ^{13}C-NMR ($CDCl_3$): δ 147.6, 147.3, 143.4, 141.03, 141.01, 138.4, 137.8, 132.7, 131.7, 130.1, 129.8, 129.5, 128.1, 127.6, 127.3, 126.2, 111.5, 109.5, 62.4, 56.0 (two overlapping signals), 55.8, 51.0, 28.8.

4-bromo-N-(4-bromobenzenesulfonyl)-N-{4'-[(6,7-dimethoxy-1,2,3,4-tetrahydroisoquinolin-2-yl)methyl]-[1,1'-biphenyl]-4-yl}benzene-1-sulfonamide (8e). $CHCl_3$. White solid. Yield:

60%. Mp (iPrOH): 228.4 - 229.2 °C. ESI^+ MS: 811 / 813 / 815 ($M+H^+$). ^{1}H-NMR ($CDCl_3$): δ 7.83 (m, 4H); 7.71 (m, 4H); 7.61 (m, 2H); 7.57 (d, *J* = 8.3 Hz, 2H); 7.5 (d, *J* = 7.9 Hz, 2H); 7.08 (m, 2H); 6.62 (s, 1H), 6.50 (s, 1H); 3.85 (s, 3H); 3.82 (s, 3H); 3.73 (s, 2H); 3.59 (s, 2H); 2.85 (t, *J* = 5.7 Hz, 2H); 2.77 (t, *J* = 5.7 Hz, 2H). ^{13}C-NMR ($CDCl_3$): δ 147.6, 147.3, 143.4, 138.8, 138.4, 132.7, 132.5, 131.7, 130.2, 129.8, 129.6, 128.1, 127.2, 126.7, 126.2, 114.0, 111.5, 109.6, 62.5, 56.0 (two overlapping peaks), 55.8, 51.0, 28.8.

N-{4'-[(6,7-dimethoxy-1,2,3,4-tetrahydroisoquinolin-2-yl)methyl]-[1,1'-biphenyl]-4-yl}-4-nitro-N-(4-nitrobenzenesulfonyl)benzene-1-sulfonamide (8f). Eluent: CH_2Cl_2 / ethyl acetate 90 / 10. White solid. Yield: 60%. Mp (iPrOH): 183.7 - 184.4 °C. ESI^+ MS: 745 ($M+H^+$). ^{1}H-NMR ($CDCl_3$): δ 8.44 (d, *J* = 8.6 Hz, 4H); 8.19 (d, *J* = 8.6 Hz, 4H); 7.65 (d, *J* = 8.3 Hz, 2H); 7.57 (d, *J* = 7.9 Hz, 2H); 7.51 (d, *J* = 7.6 Hz, 2H); 7.09 (d, *J* = 8.3 Hz, 2H); 6.62 (s, 1H); 6.50 (s, 1H); 3.85 (s, 3H); 3.82 (s, 3H); 3.74 (s, 2H); 3.59 (s, 2H); 2.85 (m, 2H); 2.77 (m, 2H). ^{13}C-NMR ($CDCl_3$): δ 151.1, 147.6, 147.4, 144.5, 140.1, 139.7, 138.0, 133.9, 131.6, 130.2, 129.9, 128.4, 127.3, 126.7, 126.3, 124.6, 111.5, 109.6, 62.5, 56.6, 56.1, 55.9, 51.0, 28.9.

[4'-(methylamino)-[1,1'-biphenyl]-4-yl]methanol (10). 4-bromo-N-methylaniline (1 mmol) (**9**), [4-(hydroxymethyl)phenyl]boronic acid (2 eq.), diisopropylamine (5 eq.) and $Pd(OAc)_2$ (0.1 eq.) were mixed in 20 mL of water. The mixture was stirred at 60 °C for 4 hours, then it was filtered through a celite pad; the pad was washed with ethyl acetate and the filtrate was further extracted with ethyl acetate; the organic phase was washed with brine, dried over Na_2SO_4, filtered and distilled under reduced pressure. The crude product was chromatographed on silica gel eluting with petroleum ether / acetone 80 / 20 to afford the product as a white solid. Yield: 74%. Mp (MeOH): 128.9 - 130.0 °C. ESI^+ MS: 214 ($M+H^+$). ^{1}H-NMR ($CDCl_3$): δ 7.56 (d, *J* = 8.3 Hz,

2H); 7.47 (d, *J* = 8.6 Hz, 2H); 7.40 (d, *J* = 8.3 Hz, 2H); 6.70 (d, *J* = 8.3 Hz, 2H); 4.72 (s, 2H); 2.89 (s, 3H). ^{13}C-NMR ($CDCl_3$): δ 148.8, 140.7, 138.5, 129.6, 127.8, 127.5, 126.4, 112.6, 65.2, 30.7.

N-[4'-(hydroxymethyl)-[1,1'-biphenyl]-4-yl]-N-methylbenzenesulfonamide (11). The compound was prepared according to the same procedure used for compounds **3a-g**. Eluent: petroleum ether / acetone 85 / 15. White solid. Yield: 60%. Mp (MeOH): 140.9 - 141.7 °C. ESI$^+$ MS: 354 ($M+H^+$). ^{1}H-NMR ($CDCl_3$): δ 7.54 (m, 11H); 7.18 (d, *J* = 8.6 Hz, 2H); 4.65 (s, 2H); 3.22 (s, 3H). ^{13}C-NMR ($CDCl_3$): δ 140.9, 140.2, 139.4, 136.8, 132.8, 129.1, 128.8, 127.8, 127.5, 127.4, 126.9, 64.9, 38.1.

General procedure for the synthesis of compounds 12a-f. Compound **3a** (0.5 mmol), the appropriate bromide reagent (2 eq.) and K_2CO_3 (3 eq.) were mixed in 20 mL of CH_3CN. The mixture was stirred at 70 °C for 16 hours. After that time the solvent was removed under reduced pressure; the residue was taken up with ethyl acetate and washed with water, brine, dried over Na_2SO_4, filtered and distilled under reduced pressure. The crude product was chromatographed on silica gel.

N-ethyl-N-[4'-(hydroxymethyl)-[1,1'-biphenyl]-4-yl]benzenesulfonamide (12a). Eluent: petroleum ether / acetone 85 / 15. Colorless oil. Yield: 84%. ESI$^+$ MS: 368 ($M+H^+$). ^{1}H-NMR ($CDCl_3$): δ 7.65 (m, 2H); 7.57 (m, 3H); 7.53 (m, 2H); 7.46 (m, 4H); 7.10 (m, 2H); 4.75 (m, 2H); 3.64 (q, *J* = 7.1 Hz, 2H); 1.82 (br. s., 1H); 1.12 (t, *J* = 7.1 Hz, 3H). ^{13}C-NMR ($CDCl_3$): δ 140.3, 19.4, 138.4, 137.9, 132.6, 129.2, 128.8, 127.63, 127.56, 127.5, 127.2, 109.9, 35.0, 45.6, 14.0.

N-butyl-N-[4'-(hydroxymethyl)-[1,1'-biphenyl]-4-yl]benzenesulfonamide (12b). Eluent: petroleum ether / acetone 85 / 15. White solid. Yield: 92%. Mp (iPrOH): 109.5 – 110.1 °C.ESI$^+$ MS: 396 (M+H$^+$). ^{1}H-NMR ($CDCl_3$): δ 7.62 (m, 2H); 7.57 (m, 3H); 7.53 (d, *J* = 8.6 Hz, 2H); 7.46 (m, 4H); 7.10 (d, *J* = 8.6 Hz, 2H); 4.75 (s, 2H); 3.56 (t, *J* = 7.1 Hz, 2H); 1.81 (br. s., 1H); 1.44 (m, 2H); 1.36 (m, 2H); 0.88 (t, *J* = 7.2 Hz, 3H). ^{13}C-NMR ($CDCl_3$): δ 140.26, 140.24, 139.4, 138.21, 138.17, 132.5, 129.0, 128.8, 127.6, 127.51, 127.46, 127.2, 65.0, 50.2, 30.2, 19.6, 13.6.

N-hexyl-N-[4'-(hydroxymethyl)-[1,1'-biphenyl]-4-yl]benzenesulfonamide (12c). Eluent: petroleum ether / acetone 90 / 10. Pale yellow oil. Yield: 59%. ESI$^+$ MS: 424 (M+H$^+$). ^{1}H-NMR ($CDCl_3$): δ 7.63 (m, 2H); 7.58 (m, 3H); 7.53 (d, 2H); 7.46 (m, 4H); 7.10 (m, 2H); 4.64 (s, 2H); 3.56 (t, *J* = 7.2 Hz, 2H); 2.00 (br. s., 1H); 1.45 (quin, *J* = 7.3 Hz, 2H); 1.33 (m, 2H); 1.24 (m, 4H); 0.85 (t, *J* = 7.1 Hz, 3H). ^{13}C-NMR ($CDCl_3$): δ 140.34, 140.28, 139.3, 138.2, 138.1, 132.5, 129.0, 128.7, 127.6, 127.5, 127.4, 127.2, 64.9, 50.5, 31.2, 26.1, 26.0, 22.4, 13.9.

N-(cyclohexylmethyl)-N-[4'-(hydroxymethyl)-[1,1'-biphenyl]-4-yl]benzenesulfonamide (12d). Eluent: petroleum ether / acetone 80 / 20. White solid. Yield: 66%. Mp (iPrOH): 126.2 – 126.8 °C ESI$^+$ MS: 436 (M+H$^+$). ^{1}H-NMR ($CDCl_3$): δ 7.59 (m, 5H); 7.53 (m, 2H); 7.46 (m, 4H); 7.11 (m, 2H); 4.76 (s, 2H); 3.38 (d, *J* = 7..2 Hz, 2H); 1.79 (m, 3H); 1.69 (dd, *J* = 12.7 Hz, 2.8 Hz, 2H); 1.62 (m, 1H); 1.36 (m, 1H); 1.13 (m, 3H); 0.988 (m, 2H). ^{13}C-NMR ($CDCl_3$): δ 140.2, 140.1, 139.4, 138.7, 138.2, 132.5, 128.9, 128.7, 127.6, 127.50, 127.47, 127.2, 65.0, 56.8, 36.9, 30.6, 26.4, 25.6.

N-benzyl-N-[4'-(hydroxymethyl)-[1,1'-biphenyl]-4-yl]benzenesulfonamide (12e). Eluent: petroleum ether / ethyl acetate 60 / 40. Off white solid. Yield: 75%. Mp (iPr_2O/iPrOH): 123.3 –

124.0 °C ESI$^+$ MS: 430 (M+H$^+$). ^{1}H-NMR (D^6-DMSO): δ 7.74 (m, 1H); 7.70 (m, 2H); 7.64 (m, 2H); 7.57 (d, *J* = 8.6 Hz, 2H); 7.56 (d, *J* = 8.6 Hz, 2H); 7.36 (d, *J* = 8.3, 2H); 7.28 (m, 4H); 7.19 (m, 1H); 7.14 (d, *J* = 8.6 Hz, 2H); 5.22 (t, *J* = 5.9 Hz, 1H); 4.84 (s, 2H); 4.52 (d, *J* = 5.5 Hz, 2H). ^{13}C-NMR (D^6-DMSO): δ 142.1, 139.0, 137.9, 137.7, 137.2, 136.3, 133.3, 129.4, 128.7, 128.4,128.0, 127.5, 127.3, 127.0, 126.8, 126.3, 62.5, 53.4.

N-[4'-(hydroxymethyl)-[1,1'-biphenyl]-4-yl]-N-[(naphthalen-1-yl)methyl]benzenesulfonamide (12f). Eluent: petroleum ether / ethyl acetate 60 / 40. Off white solid. Yield: 73%. Mp (iPr$_2$O / iPrOH): 130.5 – 131.2 °C ESI$^+$ MS: 480 (M+H$^+$). ^{1}H-NMR (D^6-DMSO): δ 8.50 (d, *J* = 8.6 Hz, 1H); 7.82 (d, *J* = 8.3 Hz, 1H); 7.77 (dd, *J* = 8.3 Hz, 1.4 Hz, 2H); 7.65 (m, 4H); 7.56 (m, 2H); 7.47 (m, 2H); 7.39 (d, *J* = 8.3 Hz, 2H); 7.33 (m, 2H); 7.20 (t, *J* = 7.6 Hz, 1H); 7.14 (d, *J* = 7.2 Hz, 1H); 6.92 (m, 2H); 5.21 (s, 2H); 4.72 (d, *J* = 5.2 Hz, 2H); 1.65 (t, *J* = 5.9, 1H). ^{13}C-NMR (D^6-DMSO): δ 140.5, 140.2, 138.3, 137.9, 137.6, 135.2, 132.9, 131.8, 129.1, 129.0, 128.9, 128.5, 128.4, 128.0, 127.7, 127.5, 127.4, 127.3, 127.2, 127.1, 126.6, 125.9, 65.0, 52.9.

General procedure for the synthesis of target compounds 14a-g. The target compounds were obtained through the same synthetic path used for compounds **5b**-**g**.

N-{4'-[(6,7-dimethoxy-1,2,3,4-tetrahydroisoquinolin-2-yl)methyl]-[1,1'-biphenyl]-4-yl}-N-methylbenzenesulfonamide (14a). Eluent: petroleum ether / acetone 80 / 20. White solid. Yield: 69%. Mp (iPrOH): 147.7 – 148.4 °C ESI$^+$ MS: 529 (M+H$^+$). ^{1}H-NMR ($CDCl_3$): δ 7.59 (m, 3H); 7.55 (m, 4H); 7.47 (m, 4H); 7.17 (m, 2H); 6.62 (s, 1H); 6.50 (s, 1H); 3.85 (s, 3H); 3.82 (s, 3H); 3.73 (s, 2H); 3.59 (s, 2H); 3.22 (s, 3H); 2.85 (t, *J* = 5.7 Hz, 2H); 2.77 (t, *J* = 5.9 Hz). ^{13}C-NMR ($CDCl_3$): δ 147.4, 147.1, 140.5, 139.9, 138.8, 138.0, 136.4, 132.8, 129.6, 128.7, 127.8, 127.4,

126.9, 126.8, 126.6, 126.1, 111.4, 109.4, 62.4, 55.9 (two overlapping signals), 55.7, 50.8, 38.1, 28.7.

N-{4'-[(6,7-dimethoxy-1,2,3,4-tetrahydroisoquinolin-2-yl)methyl]-[1,1'-biphenyl]-4-yl}-N-ethylbenzenesulfonamide (14b). Eluent: petroleum ether / acetone 80 / 20. White solid. Yield: 74%. Mp (iPrOH): 145.2 – 146.0 °C ESI$^+$ MS: 543 (M+H$^+$). ^{1}H-NMR ($CDCl_3$): δ 7.65 (dd, *J* = 8.26 Hz, 1.03 Hz, 2H); 7.57 (m, 5H); 7.47 (m, 4H), 7.11 (m, 2H); 6.62 (s, 1H); 6.50 (s, 1H); 3.85 (s, 3H); 3.82 (s, 3H); 3.73 (s, 2H); 3.65 (q, *J* = 6.9 Hz, 2H); 3.58 (s, 2H); 2.85 (t, *J* = 5.68 Hz, 2H); 2.77 (t, *J* = 5.85 Hz, 2H); 1.13 (t, *J* = 7.06 Hz, 3H). ^{13}C-NMR ($CDCl_3$): δ 147.4, 147.1, 140.4, 138.8, 138.3, 138.0, 137.7, 132.5, 129.6, 129.1, 128.8, 127.6, 127.5, 126.9, 126.6, 126.2, 111.4, 109.9, 109.4, 62.4, 55.9 (two overlapping peaks), 55.7, 50.8, 45.6, 28.7, 14.0.

N-butyl-N-{4'-[(6,7-dimethoxy-1,2,3,4-tetrahydroisoquinolin-2-yl)methyl]-[1,1'-biphenyl]-4-yl}benzenesulfonamide (14c). Eluent: petroleum ether / acetone 80 / 20. White solid. Yield: 61%. Mp (iPrOH): 100.0 – 100.6 °C ESI$^+$ MS: 571 (M+H$^+$). ^{1}H-NMR ($CDCl_3$): δ 7.63 (dd, *J* = 8.44 Hz, 1.21 Hz, 2H); 7.57 (m, 5H); 7.47 (m, 4H); 7.11 (m, 2H); 6.62 (s, 1H); 6.50 (s, 1H); 3.85 (s, 3H); 3.82 (s, 3H); 3.73 (s, 2H); 3.57 (m, 4H); 2.85 (t, *J* = 5.68 Hz, 2H); 2.77 (t, *J* = 5.85 Hz, 2H); 1.44 (m, 2H); 1.38 (m, 2H); 0.89 (t, *J* = 7.23 Hz, 3H). ^{13}C-NMR ($CDCl_3$): δ 147.5, 147.2, 140.4, 139.7, 138.8, 138.2, 138.0, 132.5, 129.6, 129.0, 128.7, 127.7, 127.5, 126.9, 126.6, 126.2, 111.4, 109.4, 62.4, 55.9, 55.7, 50.8, 50.2, 30.2, 28.7, 19.6, 13.6.

N-{4'-[(6,7-dimethoxy-1,2,3,4-tetrahydroisoquinolin-2-yl)methyl]-[1,1'-biphenyl]-4-yl}-N-hexylbenzenesulfonamide (14d). Eluent: petroleum ether / acetone 80 / 20. White solid. Yield: 84%. Mp (iPrOH): 105.3 – 106.0 °C ESI$^+$ MS: 599 (M+H$^+$). ^{1}H-NMR ($CDCl_3$): δ 7.63 (m, 2H); 7.56 (m, 5H); 7.47 (m, 4H); 7.11 (m, 2H); 6.62 (s, 1H); 6.50, (s, 1H); 3.85 (s, 3H); 3.82 (s, 3H);

3.73 (s, 2H); 3.57 (m, 4H); 2.85 (t, *J* = 5.51 Hz, 2H); 2.78 (t, *J* = 5.68 Hz, 2H); 1.45 (m, 2H); 1.34 (m, 2H); 1.24 (m, 4H); 0.86 (t, *J* = 7.06 Hz, 3H). ^{13}C-NMR ($CDCl_3$): δ 147.5, 147.2, 140.5, 140.3, 138.8, 138.2, 138.0, 132.5, 129.6, 129.0, 128.7, 127.6, 127.4, 126.9, 126.6, 126.1, 111.4, 109.4, 62.3, 55.9 (two overlapping peaks), 55.7, 50.8, 50.5, 31.2, 28.7, 28.1, 26.0, 22.5, 13.9.

N-(cyclohexylmethyl)-N-{4'-[(6,7-dimethoxy-1,2,3,4-tetrahydroisoquinolin-2-yl)methyl]-[1,1'-biphenyl]-4-yl}benzenesulfonamide (14e). Eluent: petroleum ether / acetone 80 / 20. White solid. Yield: 43%. Mp (iPrOH): 154.8 – 155.5 °C ESI$^+$ MS: 611 (M+H$^+$). ^{1}H-NMR ($CDCl_3$): δ 7.59 (m, 2H); 7.55 (m, 5H); 7.45 (m, 4H); 7.10 (m, 2H); 6.61 (s, 1H); 6.49 (s, 1H); 3.84 (s, 3H); 3.81 (s, 3H); 3.72 (s, 2H); 3.57 (s, 2H); 3.37 (d, *J* = 7.2 Hz, 2H); 2.84 (t, *J* = 5.9 Hz, 2H); 2.76 (t, *J* = 5.9 Hz, 2H); 1.77 (m, 2H); 1.68 (m, 2H); 1.61 (m, 1H); 1.35 (m, 1H); 1.12 (m, 3H); 0.96 (m, 2H). ^{13}C-NMR ($CDCl_3$): δ 147.5, 147.2, 140.2, 138.8, 138.5, 138.2, 138.0, 132.5, 129.6, 128.8, 128.7, 127.6, 127.4, 126.9, 126.6, 126.2, 111.4, 109.4, 62.4, 56.7, 55.9 (two overlapping signals), 55.7, .50.8, 35.9, 30.6, 28.7, 26.4, 25.6.

N-benzyl-N-{4'-[(6,7-dimethoxy-1,2,3,4-tetrahydroisoquinolin-2-yl)methyl]-[1,1'-biphenyl]-4-yl}benzenesulfonamide (14f). Eluent: CH_2Cl_2 / acetone 95 / 5. White solid. Yield: 86%. Mp (iPr_2O / iPrOH): 98.9 – 99.1 °C ESI$^+$ MS: 605 (M+H$^+$). ^{1}H-NMR ($CDCl_3$): δ 7.71 (m, 2H); 7.62 (m, 1H); 7.51 (m, 4H); 7.45 (m, 4H); 7.23 (m, 5H); 7.05 (m, 2H); 6.61 (s, 1H); 6.49 (s, 1H); 4.78 (s, 2H); 3.85 (s, 3H); 3.81 (s, 3H); 3.71 (s, 2H); 3.56 (s, 2H); 2.84 (t, *J* = 5.7 Hz, 2H); 2.75 (t, *J* = 5.7 Hz, 2H). ^{13}C-NMR ($CDCl_3$): δ 147.1, 140.3, 138.7, 138.6, 138.0, 137.9, 135.8, 132.7, 129.5, 129.1, 128.9, 128.5, 128.4, 127.7, 127.6, 127.4, 126.9, 126.6, 126.1, 111.4, 109.4, 62.4, 55.88, 55.86, 55.7, 54.7, 50.8, 28.7.

N-{4'-[(6,7-dimethoxy-1,2,3,4-tetrahydroisoquinolin-2-yl)methyl]-[1,1'-biphenyl]-4-yl}-N-[(naphthalen-1-yl)methyl]benzenesulfonamide (14g). Eluent: petroleum ether / acetone 70 / 30. White solid. Yield: 57%. Mp (iPrOH): 103.9 – 104.5 °C ESI^+ MS: 655 ($M+H^+$). ^{1}H-NMR ($CDCl_3$): δ 8.52 (d, *J* = 9.0 Hz, 1H); 7.81 (d, *J* = 8.3 Hz, 1H); 7.77 (dd, *J* = 8.4 Hz, 1.2 Hz, 2H); 7.66 (m, 3H); 7.53 (m, 3H); 7.44 (m, 4H); 7.35 (m, 2H); 7.19 (m, 1H); 7.13 (d, *J* = 6.2 Hz, 1H); 6.92 (m, 2H); 6.61 (s, 1H); 6.48 (s, 1H); 5.22 (s, 2H); 3.85 (s, 3H); 3.81 (s, 3H); 3.71 (s, 2H); 3.57 (s, 2H); 2.84 (m, 2H); 2.76 (m, 2H). ^{13}C-NMR ($CDCl_3$): δ 147.5, 147.2, 140.2, 138.7, 137.8, 137.4, 133.6, 132.9, 131.7, 130.4, 129.5, 129.1, 128.9, 128.8, 128.5, 128.4, 128.1, 127.9, 127.1, 126.8, 126.6, 126.0, 125.9, 125.8, 124.8, 124.0, 111.3, 109.4, 62.1, 55.8 (two overlapping peaks), 55.5, 52.9, 50.7, 29.2.

BIOLOGY

Materials. Cell culture reagents were purchased from Celbio s.r.l. (Milano, Italy). CulturePlate 96/wells plates were purchased from PerkinElmer Life Science (Waltham, MA) and Falcon (BD Biosciences, Bedford, MA). Calcein-AM, bisBenzimide H 33342 trihydrochloride were obtained from Sigma-Aldrich (Milan, Italy). Electrophoresis reagents were from Bio-Rad Laboratories (Hercules, CA). The protein content of cell monolayers and cell lysates was assessed with the bicinchoninic acid kit (Sigma Aldrich). The other reagents were purchased from Sigma Merck Millipore.

Cell cultures. MDCK-MDR1, MDCK-MRP1 and MDCK-BCRP cells are a gift of Prof. P. Borst, NKI-AVL Institute, Amsterdam, The Netherlands. Caco-2 cells were a gift of Dr. Aldo Cavallini and Dr. Caterina Messa from the Laboratory of Biochemistry, National Institute for Digestive Diseases, “S. de Bellis”, Bari (Italy). Cells were grown in DMEM high glucose

supplemented with 10% fetal bovine serum, 2 mM glutamine, 100 U/mL penicillin, 100 μg/mL streptomycin, in a humidified incubator at 37 °C with a 5 % CO_2 atmosphere.

Co-administration Assay. The co-administration assay with Doxorubicin was performed in MDCK-MDR1 cells at 48h as reported with minor modification.[25] On day 1, 10000 cells/well were seeded into 96-well plates in a volume of 100 μL of fresh medium. On day 2, the tested drug was added alone to the cells at different concentrations (10 nM, 100 nM, 1 μM). On day 3, the medium was removed and the drug at the same concentrations was added alone and in co-administration with 10 μM Doxorubicin to the cells. After the established incubation time with the tested drug, MTT (0.5 mg/mL) was added to each well, and after 3-4 h incubation at 37 °C, the supernatant was removed. The formazan crystals were solubilized using 100 μL of DMSO/EtOH (1:1), and the absorbance values at 570 and 630 nm were determined on the microplate reader Victor 3 from PerkinElmer Life Sciences.

Caco-2 monolayer preparation. For permeability and drug transport assays, to prepare the Caco-2 monolayer, considered an in vitro model of GI barrier,[1] cells were seeded into a Millicell® Transwell assay system (Millipore, Bedford, MA), where a cell monolayer is set in between a filter cell and a receiver plate, at a density of 10,000 cells/well.[12] The culture medium was replaced every 48 h and the cells kept for 21 days in culture. The Trans Epithelial Electrical Resistance (TEER) of the monolayers was measured daily, before and after the experiment, using an epithelial voltohmmeter (Millicell® -ERS, Millipore). Generally, TEER values greater than 1000 Ω for a 21 day culture are considered optimal.

Immunoblotting. Cells were lysed in MLB buffer (125 mM Tris-HCl, 750 mM NaCl, 1% v/v NP40, 10% v/v glycerol, 50 mM $MgCl_2$, 5 mM EDTA, 25 mM NaF, 1 mM $NaVO_4$, 10 mg/ml

leupeptin, 10 mg/ml pepstatin, 10 mg/ml aprotinin, 1 mM phenylmethylsulphonyl fluoride, pH 7.5), sonicated and centrifuged at 13,000 g for 10 min at 4°C. 50 μg of proteins were subjected to immunoblotting and probed with the following antibodies: anti-ABCB1/P-gp (C219, Novus Biologicals, Littleton, CO, dilution 1/250), anti-ABCC1/MRP1 (IU2H10, Abcam, Cambridge, UK, dilution 1/100), anti-ABCG2/BCRP (sc-25882, Santa Cruz Biotechnology Inc., Santa Cruz, CA, dilution 1/500), followed by a peroxidase-conjugated secondary antibody. Proteins were detected by enhanced chemiluminescence (Bio-Rad Laboratories).

Permeability assays of luciferin yellow, sulforhodamine B and FITC-insulin gastro-intestinal barrier. After 21 days of culture in the conditions reported above, the medium was removed from filter wells and from the receiver plate, which were filled with fresh HBSS buffer (Invitrogen). This procedure was repeated twice, and the plates were incubated at 37 °C for 30 min. After incubation time, the HBSS buffer was removed. 100 μM of luciferin yellow, sulforhodamine B, fluorescein isothiocyanate (FITC)-insulin, i.e. molecules with a low transport across a competent GI barrier,[29,30] all dissolved in HBSS, were added in the filter of each Transwell, while fresh HBSS was added to the receiver plate. The plates were incubated at 37 °C for 120 min. Afterwards, samples were removed from the apical (filter well) and basolateral (receiver plate) side of the monolayer to measure the permeability. The concentration of luciferin yellow, sulforhodamine B and FITC-insulin was measured spectrofluorimetrically, using a Synregy HTX 96-well plate reader (Bio-Tek Instruments, Winooski, VT), according to the previously set calibration curves, using the following wavelengths: excitation 318 nm, emission 518 (luciferin yellow),[29] excitation 560 nm, emission 590 (sulforhodamine B),[30] excitation 488 nm, emission 525 (FITC-insulin).[30]

The apparent permeability (P_{app}), in units of nmol/second, was calculated using the following equation:

$$P_{app} = \left(\frac{V_A}{\text{Area} \times \text{time}} \right) \times \left(\frac{[\text{drug}]_{\text{acceptor}}}{[\text{drug}]_{\text{initial}}} \right)$$

VA = the volume (1 mL) in the acceptor well;

Area = the surface area of the membrane (0.11 cm^2 of the well);

time = the total transport time in seconds (7200 sec);

[compound]acceptor = the concentration of the compound in the receiver compartment

[compound]initial = the initial concentration in the apical or basolateral wells.

Calcein-AM experiments. These experiments were carried out as described by Riganti et al. with minor modifications.[25] Each cell line (30,000 cells per well) was seeded into black CulturePlate 96/wells plate with 100 µL medium and allowed to become confluent overnight. 100 µL of test compounds were solubilized in culture medium and added to monolayers, with final concentrations ranging from 0.1 to 100 µM. 96/Wells plate was incubated at 37 °C for 30 min. Calcein-AM was added in 100 µL of Phosphate Buffered Saline (PBS) to yield a final concentration of 2.5 µM and plate was incubated for 30 min. Each well was washed 3 times with

ice cold PBS. Saline buffer was added to each well and the plate was read with Victor3 (PerkinElmer) at excitation and emission wavelengths of 485 nm and 535 nm, respectively. In these experimental conditions Calcein cell accumulation in the absence and in the presence of tested compounds was evaluated and fluorescence basal level was estimated with untreated cells. In treated wells the increase of fluorescence with respect to basal level was measured. EC_{50} values were determined by fitting the fluorescence increase percentage versus log[dose].

Hoechst 33342 experiment. These experiments were carried out as described by Riganti et al. with modifications.[25] Each cell line (30,000 cells per well) was seeded into black CulturePlate 96/wells plate with 100 μL medium and allowed to become confluent overnight. 100 μL of test compounds were solubilized in culture medium and added to monolayers, with final concentrations ranging from 0.1 to 100 μM. 96/Wells plate was incubated at 37 °C for 30 min. Hoechst 33342 was added in 100 μl of Phosphate Buffered Saline (PBS) to yield a final concentration of 8 μM and plate was incubated for 30 min. The supernatants were drained and the cells were fixed for 20 min under light protection using 100 μL per well of a 4% PFA solution. Each well was washed 3 times with ice cold PBS. Saline buffer was added to each well and the plate was read with Victor3 (PerkinElmer) at excitation and emission wavelengths of 340/35 nm and 485/20 nm, respectively. In these experimental conditions, Hoechst 33342 accumulation in the absence and in the presence of tested compounds was evaluated and fluorescence basal level was estimated with untreated cells. In treated wells the increase of fluorescence with respect to basal level was measured. EC_{50} values were determined by fitting the fluorescence increase percentage versus log[dose].

ATPlite assay. The MDCK-MDR1 cells were seeded into 96-well microplate in 100 μL of complete medium at a density 2 × 104 cells/well.[25] The plate was incubated overnight (O/N) in a humidified atmosphere 5% CO_2 at 37 °C. The medium was removed and 100 μL of complete medium either alone or containing different concentrations of test compounds was added. The plate was incubated for 2h in a humidified 5% CO_2 atmosphere at 37 °C. 50 μL of mammalian cell lysis solution was added to all wells and the plate shaked for five minutes in an orbital shaker. 50 μL of substrate solution was added to all wells and the plate shaked for five mitutes in an orbital shaker. The plate was dark adapted for ten minutes and the luminescence was measured.

Drug transport assays. After 21 days of Caco-2 cell growth in Transwell systems, the medium was removed from filter wells and from the receiver plate and substituted with HBSS buffer twice. The plates were incubated at 37 °C for 30 min, then 1 μCi of the following drugs, substrates of P-gp, was added to the receiver plate, in the absence (Ctrl) or presence of 100 nM of the ligand **8b**: [^{3}H]-digoxin (PerkinElmer), [^{3}H]-quinidine (Biotrend, Koln, Germany), [^{3}H]-prazosin (PerkinElmer), [^{3}H]-carbamazepine (Biotrend), [^{3}H]-imipramine (Biotrend), [^{3}H]-lansoprazole (Biotrend), [^{3}H]-ritonavir (Biotrend), [^{3}H]-rifampicin (Biotrend), [^{3}H]-dexamethasone (Biotrend), [^{3}H]-tamoxifen (Biotrend). After 2 h at 37°C, the concentration of each drug was measured in the basolateral compartment by liquid scintillation, by adding 2 mL UltimaGold amplifier (PerkinElmer) to each sample, according to the relative calibration curve. The counts per minutes (cpm) were recorded; the results were expressed as percentage of cpm in each sample treated with the inhibitor versus the cpm in the samples without the inhibitor (Ctrl).

ATPase assay. P-gp and MRP1 were immuno-precipitated from 100 μg of membrane–associated proteins, then the rate of ATP hydrolysis, an index of the catalytic cycle and a necessary step for substrate efflux, was measured spectrophotometrically.[31] Results were expressed as nmol hydrolyzed phosphate/mg protein.

Viability assay. Determination of cell growth was performed using the MTT assay at 48 h and 72 h.[32] On day 1, 10000 MDCK cells or Caco-2 cells/well were seeded into 96-well plates in a volume of 100 μL. On day 2, the inhibitor was added at different concentration. In all the experiments, the various drug-solvents (ethanol, DMSO) were added in each control to evaluate a possible solvent cytotoxicity. After the established incubation time with drugs, MTT (0.5 mg/mL) was added to each well, and after 3 h incubation at 37°C, the supernatant was removed. The formazan crystals were solubilized using 100 μL of DMSO and the absorbance values at 570 and 630 nm were determined on the microplate reader Victor 3 (PerkinElmer).

In vitro simulated digestion. Saliva, gastric fluid and duodenal fluid were prepared according to.[32] To mimic the steps of the physiological digestion, 1 μM compound (final volume: 0.1 mL) was incubated for 5 min at 37°C in 0.3 mL saliva (pH 6.8), then 0.6 mL of gastric fluid were added for 2 h at 37°C (pH 1.3) under shaking, followed by 0.6 mL of duodenal fluid (pH 8.1) for 2 h at 37°C under shaking.[32] The digested compound was then diluted 1:10 in cell culture medium of the Transwell insert. In this experimental conditions, the viability of Caco-2 cells incubated with the digested compound did not differ from the viability of the cells incubated with the pristine compound (not shown).

Statistical analysis. All data in the text and figures are provided as means ± SEM. The results were analysed by a Student's t-test and ANOVA test, using Graph-Pad Prism (Graph-Pad software, San Diego, CA, USA). $p < 0.05$ was considered significant.

RESULTS AND DISCUSSION

CHEMISTRY

The target compounds were synthesized according to the path reported in scheme 1. Almost all of the compounds were obtained starting from derivative **2**, that in turn was prepared according to a reported procedure.[25] Compound **2** was reacted with the appropriate sulfonyl chloride and pyridine at room temperature, to afford the corresponding sulfonamides **3a**-**g**. The latter ones were converted to benzylic chlorides, with thionyl chloride, and promptly reacted with 6,7-dimethoxy-1,2,3,4-tetrahydroisoquinoline hydrochloride in basic conditions, to give target compounds **5b**-**g** in moderate to good yields (31 – 87%). The N-sulfonylsulfonamide-compounds **8b**-**f** were obtained starting from intermediates **3b**-**f**: the latter ones were sulfonylated with the appropriate sulfonyl chloride and triethylamine at 70 °C. The benzylic alcohols **6b**-**f** were converted to the corresponding chlorides and then to target compounds **8b**-**f**, with the same reaction conditions used for the first series (yields: 60 – 78%).

As for the N-alkylsulfonamide- series, the N-methyl derivative was obtained starting from the commercially available 4-bromo-N-methylaniline, which was converted to **10** through Suzuki coupling reaction with [4-(hydroxymethyl)phenyl]boronic acid and $Pd(OAc)_2$ in water. The N-methylaniline **10** was sulfonylated with benzenesulfonyl chloride in the usual conditions. The remainder N-alkylsulfonamide- derivatives were obtained starting from the common intermediate **3a** through alkylation with the appropriate bromides in basic condition. The

benzylic alcohols **11** and **12a-f** thus obtained were activated with thionyl chloride and reacted with 6,7-dimethoxy-1,2,3,4-tetrahydroisoquinoline hydrochloride to afford the target compounds **14a-g** in moderate to high yields (43 – 86%).

Scheme 1. Synthesis of target compounds.

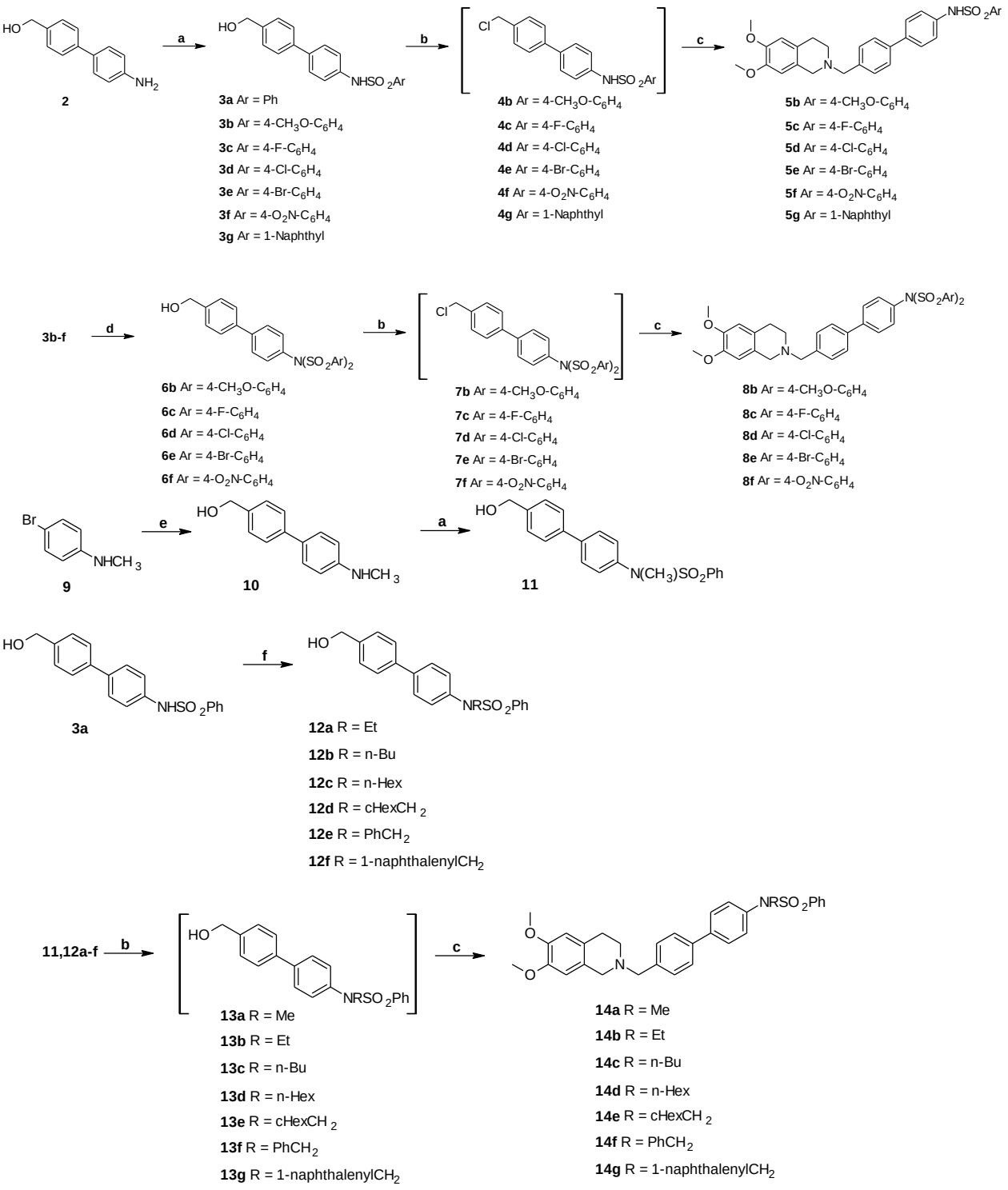

Reagents and conditions. (a) Arylsulfonyl chloride, pyridine, CH_2Cl_2 room temperature, 6 hours; (b) $SOCl_2$, pyridine, tetrahydrofuran, room temperature, 1 hour; (c) 6,7-dimethoxy-1,2,3,4-tetrahydroisoquinoline hydrochloride, 1,5-diazabicyclo(5.4.0)undec-7-ene (DBU), CH_3CN, 70 °C, 8 hours; (d) arylsulfonyl chloride, Et_3N, CH_3CN, 70 °C, 16 hours; (e) [4-(hydroxymethyl)phenyl]boronic acid, $(iPr)_2NH$, $Pd(OAc)_2$, H_2O, 60 °C, 4 hours; (f) RBr, K_2CO_3, CH_3CN, 70 °C, 16 hours.

BIOLOGY

P-gp Interacting Profile and ABC Transporters Selectivity

As already reported in our previous study[25], for all the synthesized compounds three combined assays have been performed to establish the P-gp interacting mechanism and the selectivity versus P-gp: 1) the inhibition of the transport of a profluorescent probe that is also a P-gp substrate, Calcein-AM, in a cell line overexpressing P-gp (MDCK-MDR1 cells); 2) the determination of the Apparent Permeability parameter P_{app} in a Caco2 cells monolayer; 3) the measure of ATP cell depletion in the same cell line overexpressing P-gp (MDCK-MDR1 cells). The first assay gives us the measure of the ligand potency vs P-gp and the same strategy was used to study the selectivity of all compounds vs P-gp, since it was used to evaluate the activity also vs MRP1 and BCRP. Indeed, the calcein-AM is also a MRP1 substrate and may be used in the transport inhibition assay in a cell line overexpressing MRP1 (MDCK-MRP1 cells); while to measure the effect of the ligands vs BCRP, the inhibition of a BCRP substrate, Rhodamine123, was probed in a cell line overexpressing BCRP (MDCK-BCRP cells). From the combination of these three assays, a P-gp ligand can be classified as depicted in Table 1 as P-gp unambiguous substrate, P-gp inhibitor, or a P-gp ambiguous substrate. The substrates may be also differently categorized on the basis of the different effect on ATP cell level.[12]

Table 1. P-gp ligands classification on the basis of the three biological assays.

P-gp ligands	**Papp**	**ATP cell depletion**	**Substrate transport inhibition**
Unambiguous nonsubstrates	<2	No	No
Unambiguous substrates	>2	Yes	Yes

Inhibitors	<2	No	Yes

All the synthesized ligands reported in Table 2 were inspired by the lead compound **5b,** previously developed, displaying a very high P-gp potency (EC_{50} = 15.3 nM) and selectivity (as not active towards MRP1 and BCRP). All the planned modification led to compounds displaying a decreased activity vs the pump P-gp with respect to the lead compound **5b**, but high selectivity, as the lead compound. Among all the ligands, compound **8b** emerges as a P-gp ligand endowed with high potency, in the nanomolar range, and high selectivity, since inactive vs MRP1 and BCRP. For this reason, it was tested in a preliminary study to probe its usefulness to improve the bioavailability of drugs normally effluxed by P-gp.

Table 2. Biological Activity Profile of Target Compounds.

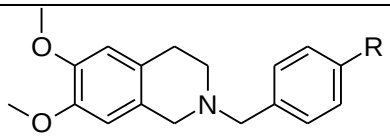

Cmpd. No	**R**	**EC_{50} ± SEM (μM)[a]**			**BA/AB[b]**	**ATP**
		MDR1	**MRP1**	**BCRP**		
1[25]	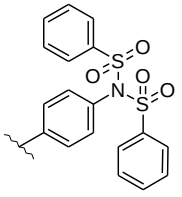	0.015	NA	NA	>20	NO
5b	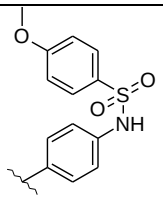	0.74	NA	NA	11.3	NO

8b	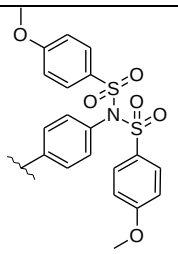	0.094	NA	NA	9.5	NO
5c	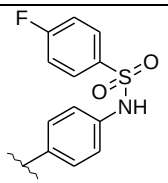	0.94	NA	NA	34	NO
8c	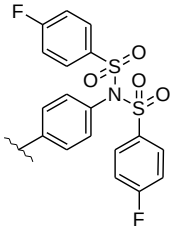	0.74	NA	NA	13.5	NO
5d	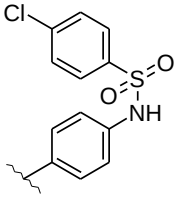	2.16	NA	NA	14.35	NO
8d	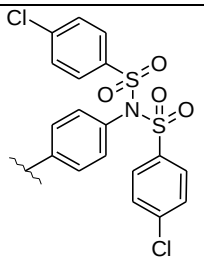	7.0	NA	NA	164	NO
5e	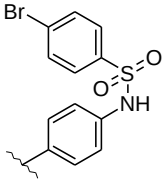	2.6	NA	NA	14.97	NO
8e	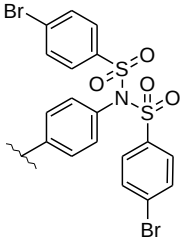	0.98	NA	NA	4.07	NO

5f	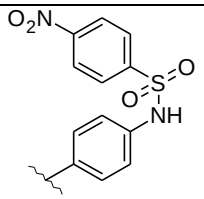	3.2	NA	NA	9.88	NO
8f	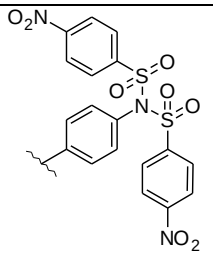	1.12	NA	NA	10.77	NO
5g	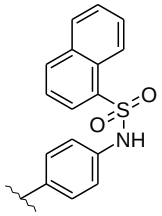	1.07	NA	NA	14.3	NO
14a	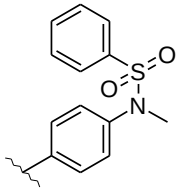	0.43	NA	NA	37	NO
14b	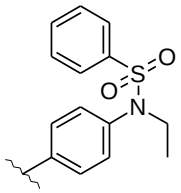	0.28	NA	NA	15.4	NO
14c	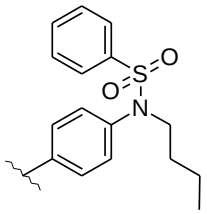	0,63	NA	NA	3.3	NO
14d	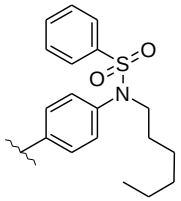	1.1	NA	NA	4.8	NO

14e	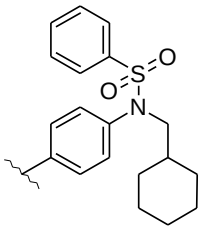	3	NA	NA	38.5	NO
14f	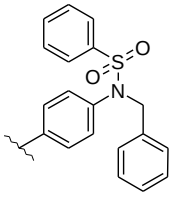	1.3	NA	NA	21.8	NO
14g	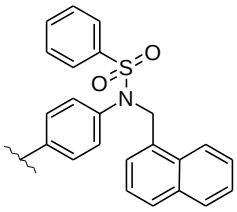	3.5	NA	NA	3.6	NO

[a] Values are the means ± SEM of three independent experiments carried out in triplicate.

[b] Apparent permeability ratio (the value is from two independent experiments).

Co-administration assay with the antineoplastic drug Doxorubicin

A preliminary screening of the ability of **8b** to reduce P-gp activity restoring the cytotoxic effects of the antineoplastic drug Doxorubicin, a typical P-gp substrate, was measured in MDCK-MDR1 cells. As depicted in Figure 1, Doxorubicin and compound **8b**, tested alone, were both not cytotoxic vs MDCK-MDR1cells, since Doxorubicin was not able to exert its anticancer activity as it was effluxed by P-gp and compound **8b** was not cytotoxic *per se*.

The 10 μM concentration of Doxorubicin was chosen after a preliminary test performed with different dosages (data not shown). Compound **8b** was probed at concentrations ranging from its EC_{50} value (around 100 nM) to a 10-fold more concentrated value (1 μM).

As depicted in Figure 1, when the antineoplastic drug was co-administered with compound **8b**, its cytotoxic effect was significantly increased at all the tested concentrations of **8b** exerting the maximum cytotoxic activity (around 50%) in the presence of 500 nM and 1 μM compound **8b**. This finding suggests the use of compound **8b** can be a winning strategy to improve the bioavailability of other substrates of P-gp. Since P-gp is abundantly expressed on the luminal side of epithelial colon cells, we next focus on GI barrier and on the potential impact of compound **8b** on the transport of different orally administered drugs, all substrates of P-gp.

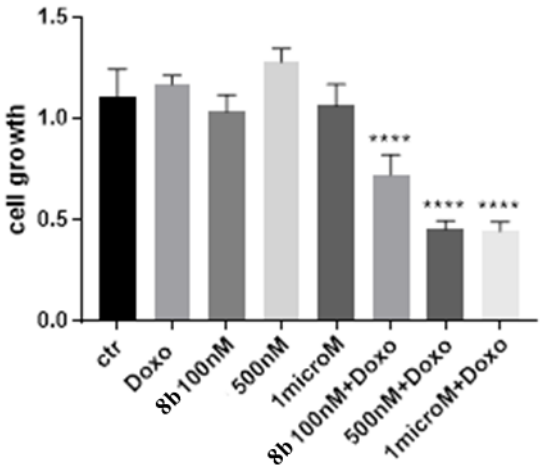

Figure 1. Antiproliferative activity on MDCK-MDR1 cells of Doxorubicin at 10 μM and compound **8b** at 100nM, 500nM and 1μM, alone and in co-administration with Doxorubicin 10 μM. Each bar represents the mean ± SEM of two experiments performed in triplicate. One-way analysis of variance (ANOVA) analysis: ****$p < 0.0001$ vs control.

Compound 8b does not alter the physiological properties of Caco-2 cells barrier model

To investigate the potential of compound **8b** to inhibit P-gp in intestinal cells, we first set up a reliable GI barrier model by culturing 21 days human Caco-2 until the formation of a competent

monolayer.[1] After this time, TEER value was 175 ± 36 Ω cm^2, in line with the values reported for a competent GI model.[29] Moreover, we measured the apical-to-basal permeability of three molecules of different molecular weights: luciferin yellow and sulforhodamine B, two fluorescent tracers characterized by low molecular weight[29,30], and FITC-insulin[30], a macromolecule with higher molecular weight. The values are reported in Table 3, and are in the same ranges of other Caco-2-based GI models.[29,30]

Table 3. P_{app} of luciferin yellow, sulforhodamine B and FITC-insulin across Caco-2 monolayer.

P_{app}	**(nmol/s)**
Luciferin Yellow	2.54 ± 0.29
Sulforhodamine B	2.47 ± 0.14
FITC-Insulin	0.13 ± 0.05

Caco-2 cells were seeded in Transwell systems for 21 days, then incubated 2 h with 100 μM luciferin yellow, sulforhodamine B and FITC-inulin in the receiver plate. The concentrations in donor and receiver compartment were measured fluorimetrically, and used to calculate P_{app}. Data are means ± SEM.

A competent GI barrier usually have no permeability to proteins, included insulin, and have a very low permeability to the small molecules luciferin yellow and sulforhodamine B.[29,30] All these molecules are transported paracellularly[1]: an increase in their permeability is indicative of disruption of TJs complexes and substrates leakage across Caco-2 monolayer. Our results of TEER and permeability assays indicate instead a competent GI barrier in our experimental conditions.

Caco-2 cells are reported to express different ABC transporters, including P-gp, cultured either as undifferentiated cells[33] or as GI barrier.[34] As shown in Figure 2, our Caco-2 cells after 21 days of culture express P-gp and MRP1, at lower level than MDCK-P-gp and MDCK-MRP1, used as internal positive control. By contrast, Caco-2 cells do not express BCRP. These data suggest that our experimental model can be used to test the efflux activity of P-gp and MRP1 transporters, in a competent GI barrier.

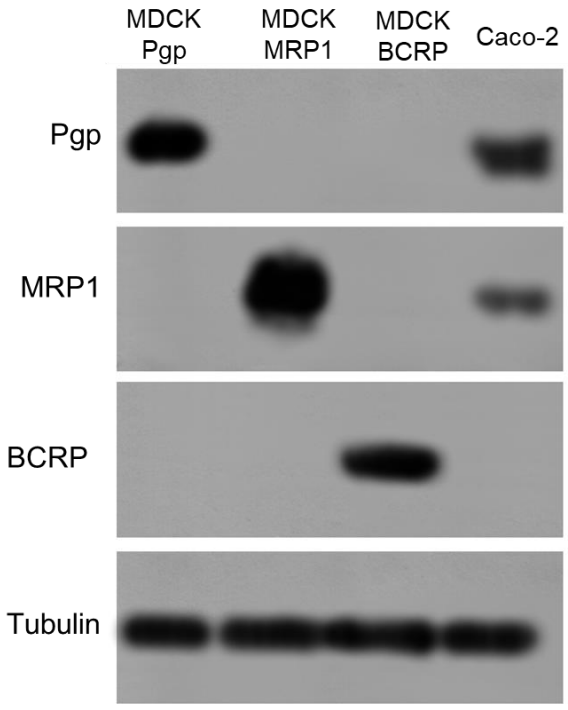

Figure 2. Immunoblot of the indicate proteins in Caco-2 cells monolayer, after 21 days of culture in Transwell. MDCK-MDR1, MDCK-MRP1 and MDCK-BCRP cells were used as positive controls of cell lines expressing the relative proteins. Tubulin was used as control of equal proteins loading. The figure is representative of one out of three experiments

We next tested the impact of compound **8b** on cell viability, TEER and transport properties of Caco-2 cells. As reported in Figure 3, compound **8b** displayed a dose-dependence cytotoxicity

that was significant at $\geq$ 10 μM concentration. Notably, at 100 nM, i.e. a concentration similar to the EC_{50} value, compound **8b** did not reduce cell viability. According to this result, we used the compound at 100 nM for all the following experiments.

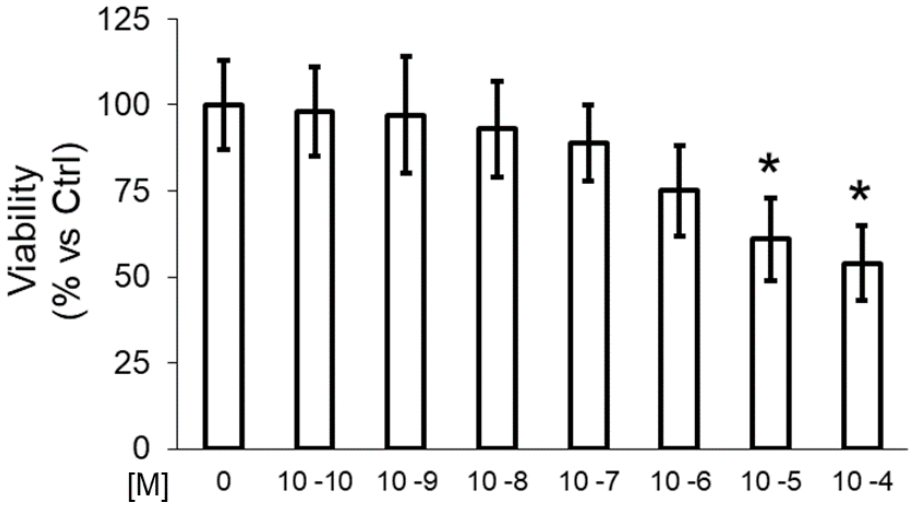

Figure 3. Caco-2 viability of cells incubated with compound **8b** at different concentrations (10^{-10} - 10^{-4} M). Control cells (0) were grown in fresh medium and their viability was considered 100%. Each bar represents the mean ± SEM of four experiments performed in triplicate. One-way analysis of variance (ANOVA) analysis: *$p < 0.05$ vs control cells.

In this condition TEER value of Caco-2 cells incubated with the compounds for 2 h was 176 $\pm$ 32 Ω cm^2, compared to the TEER value of Caco-2 cells grown in fresh medium, used as control of this experimental set, of 181 $\pm$ 41 Ω cm^2. Similarly, compound **8b** did not alter the P_{app} of luciferin yellow, sulforhodamine B and FITC-inulin compared to the control values (Table 4).

Table 4. Effect of compound 8b on the P_{app} of luciferin yellow, sulforhodamine B and FITC-insulin.

Substrate	P_{app} (nmol/s)	
	- 8b	+ 8b
Luciferin Yellow	2.29 ± 0.36	2.38 ± 0.15
Sulforhodamine B	2.12 ± 0.23	2.24 ± 0.13
FITC-Insulin	0.15 ± 0.04	0.12 ± 0.06

Caco-2 cells were seeded in Transwell systems for 21 days, then incubated 2 h with fresh medium (-) or 100 nM compound **8b** (+), in the presence of 100 μM luciferin yellow, sulforhodamine B and FITC-inulin in the receiver plate. The concentrations in donor and receiver compartment were measured fluorimetrically, and used to calculate P_{app}. Data are means ± SEM.

These results suggest that compound **8b** may have a good biocompatibility, because it produces a modest but significant toxicity only at high micromolar concentrations that are difficultly reached in vivo, with the compound administered *per os*. Most importantly, at a concentration similar to the EC_{50} displayed on P-gp, the compound does not alter the electro-physiological property of GI barrier, as indicated by the values of TEER and of permeability of biomolecules usually poorly transported across the GI barrier.

Compound 8b selectively reduces the activity of P-gp and increases the transport of multiple P-gp substrates across gastro-intestinal barrier

We next investigated whether compound **8b** effectively inhibited the catalytic function of P-gp in our model of GI barrier. At 100 nM the compound significantly reduced the ATPase catalytic activity of immunopurified P-gp extracted from Caco-2 monolayer (Figure 4A). This inhibition was specific, since MRP1 activity was unchanged (Figure 4B). The change in the protein activity

was not due to a change in protein expression (Figure 4C) but was probably mainly due to the P-gp interacting mechanism previously underlined.

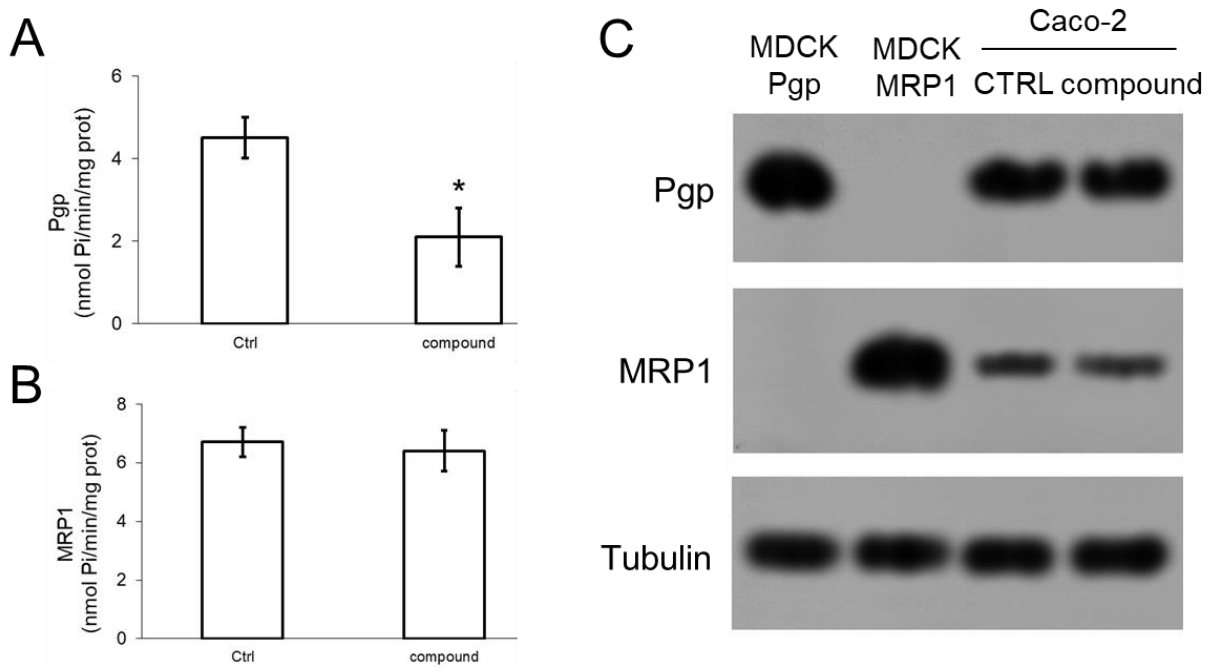

Figure 4. Effect of compound 8b on ATPase activity and expression of P-gp and MRP1. Caco-2 cells, cultured 21 days in Transwell devices, were incubated in fresh medium or with 100 nM compound **8b** for 2 h. A-B. P-gp and MRP1 ATPase activity, measured spectrophotometrically on the immuno-purified proteins. Each bar represents the mean ± SEM of four experiments performed in triplicate. One-way analysis of variance (ANOVA) analysis: *$p < 0.005$ vs Ctrl cells. C. Immunoblot of the indicated proteins in Caco-2 cells, treated as reported above, and in MDCK-P-gp and MDCK-MRP1 cells, used as positive controls. Tubulin was used as control of equal proteins loading. The figure is representative of one out of three experiments.

Finally, we evaluated if the compound **8b** may increase the apical-to-basal transport of drugs that are known substrates of P-gp and are commonly orally assumed. We tested the transport of the following radiolabeled drugs meeting the above requisites: digoxin[35], used in the treatment of

chronic heart failure; the anti-arrhythmic agent quinidine[36], the anti-hypertensive drug prazosin[37], the anti-convulsive drug carbamazepine[38], the anti-depressant agent imipramine[39], the anti-acid agent lansoprazole[40], the anti-retroviral agent ritonavir[41], the antibiotic rifampicin[42], the anti-inflammatory agent dexamethasone[43], the anti-estrogen drugs tamoxifen.[44] These drugs were chosen among the P-gp substrates, from the DrugBank entry https://www.drugbank.ca/categories/DBCAT002668, in order to have different classes of agents, prescribed for common diseases. In all cases, compound **8b** increased the apical-to-basal transport across the Caco-2 monolayer (Figure 5).

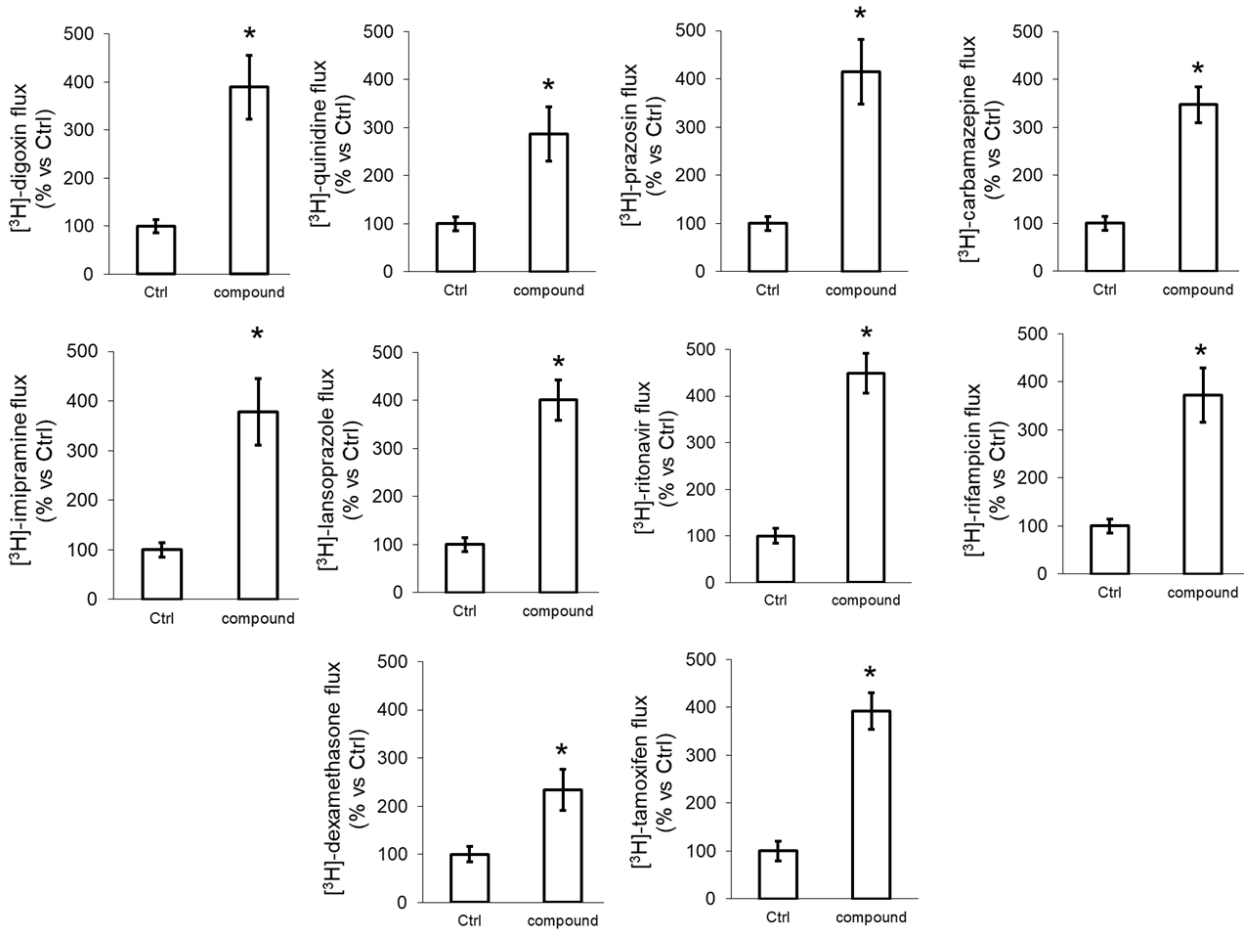

Figure 5. Effect of compound 8b on P-gp mediated transport of selected drugs. Caco-2, cultured 21 days in Transwell devices, were incubated in fresh medium (Ctrl) or with 100 nM compound **8b** for 2 h, in the presence of 1 μCi of the indicated drugs. The radioactivity of the lower chamber, considered an index of the apical-to-basal transport, was measured by liquid scintillation in duplicate. Each bar represents the mean ± SEM of three experiments performed in triplicate. One-way analysis of variance (ANOVA) analysis: *$p < 0.001$ vs Ctrl cells.

The localization on the luminal side of the intestinal cells makes P-gp the main transporter for several drugs orally taken. The efflux activity, followed by the fecal excretion of the drugs, results in lower bioavailability of the drug and consequent lower efficacy.[5] Although obtained in vitro, our data suggest that compound **8b** may potentially increase the bioavailability of several commonly prescribed drugs, different for structures and indications, but sharing the property of being actively transported by P-gp. Moreover, at the concentration used, the compound is not toxic for GI barrier cells. We can hypothesize that the compound **8b**, co-administerd with specific drugs, may even reduce the dosage of the drugs administered, limiting the side-effects and maximizing the therapeutic benefits. We are aware that one of the main limitations of P-gp inhibitors has been the unexpected toxicity and drug-drug interactions between the inhibitor and the P-gp substrate.[45] We are evaluating this issue in mice receiving compound **8b** and specific drugs tested in the present work, with the aim of investigating if our new P-gp inhibitor may improve their oral bioavailability without exerting undesired toxicities in vivo.

Furthermore, compounds taken by the oral route may be altered after the digestion, because of the passage in GI tract with different pH and osmolarity. We have thus investigated if the compound retains its properties after in vitro simulated digestion protocols, reproducing the timing, pH and osmolarity conditions of the digestive fluids, including saliva, gastric fluid and

duodenal fluid.[32] After the simulated digestion in vitro, the compound still retained its ability to inhibit P-gp activity, as the pristine compound (Figure 6A). Accordingly, it maintained the same ability to increase the transport of digoxin, a classical substrate of P-gp, across competent Caco-2 barrier (Figure 6B).

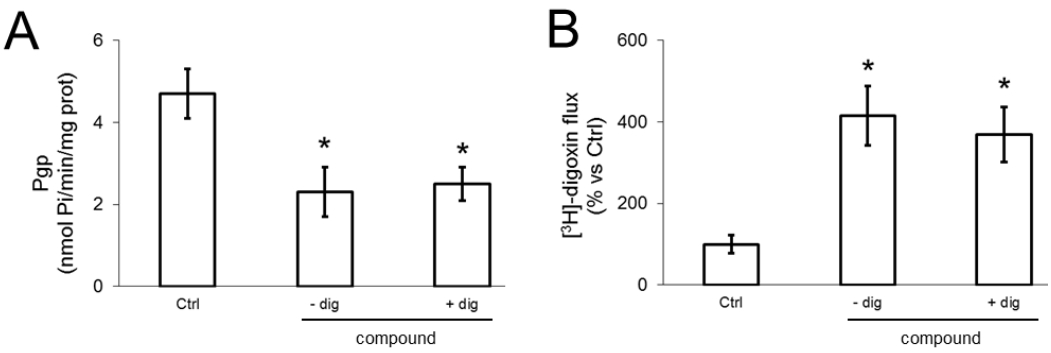

Figure 6. Activity of compound 8b after simulated in vitro digestion. Caco-2 cells, cultured 21 days in Transwell devices, were incubated for 2 h in fresh medium (Ctrl) or with 100 nM compound **8b**, directly (- dig) or after pre-treatment with gastrointestinal fluids (+ dig). A. P-gp ATPase activity, measured spectrophotometrically on the immuno-purified proteins. Each bar represents the mean ± SEM of four experiments performed in triplicate. One-way analysis of variance (ANOVA) analysis: *$p < 0.005$ vs Ctrl cells. B. 1 μCi of [^{3}H]-digoxin was co-incubated in the upper chamber. The radioactivity of the lower chamber, considered an index of the apical-to-basal transport, was measured by liquid scintillation in duplicate. Each bar represents the mean ± SEM of three experiments performed in triplicate. One-way analysis of variance (ANOVA) analysis: *$p < 0.001$ vs Ctrl cells.

These results suggest that the compound does not lose its functional properties after the transit through the GI fluids, therein it may be reasonably administered *per os* still maintaining the property of increasing the bioavailability of other drugs substrates of P-gp, administered *per os*.

The amount and activity of P-gp vary from 2 to 8 fold inter-individually.[42] Moreover, P-gp polymorphisms can change the catalytic efficiency of the protein, sometimes enhancing the efflux activity.[46] This is another factor increasing the variability of the oral bioavailability of drugs. Our results demonstrates that compound **8b** was active in cells with different levels of P-gp, i.e. Caco-2 and MDCK-MDR1 cells, indicating that it has the potential to inhibit P-gp expressed at different amount. Analyzing if it is active on cells with different P-gp variants, by checking the efflux activity in cells ectopically expressing different polymorphic variants of P-gp, will represent the next step of investigation, in order to identify potential subsets of patients who may most benefit from our inhibitor.

CONCLUSIONS

Besides being a physiological mechanism of defense, P-gp mediated transport of structurally diverse molecules is a well-established cause of cancer chemotherapy failure and lower drug bioavailability at physiological barrier. For instance, P-gp activity at the GI barrier is responsible for low and/or unpredictable bioavailability of a number of orally administered drugs belonging to different therapeutic areas. The present work gives a promising perspective for both fronts: compound **8b**, the result of the ongoing efforts of the authors in the search of effective P-gp ligands, is able to inhibit P-gp activity at nanomolar concentrations. Owing to its molecular mechanism of action, it is effective in restoring cytotoxic activity of Doxorubicin, appearing promising in increasing the efficacy of chemotherapeutic drugs in P-gp-expressing tumors. Moreover it is able to increase the delivery across the GI barrier of several drugs, potentially inducing a greater bioavailability after oral administration, without perturbing the functional features of the barrier and without losing its efficacy following to contact with digestive fluids. These results will be complemented by future investigations aimed at verifying the

pharmacokinetic profile of compound **8b** and the co-administered drug, and giving a clear picture of the influence on the efficacy of **8b** exerted by individual variability, in terms of P-gp expression and polymorphism.

AUTHOR INFORMATION

Corresponding Authors

SG: stefano.guglielmo@unito.it

CR: chiara.riganti@unito.it

Author Contributions

The manuscript was written through contributions of all authors. All authors have given approval to the final version of the manuscript.

Funding Sources

This study was supported by the University of Turin – "Ricerca Locale", by MIUR (grant GUGS_FFABR_17_01 to SG; by Associazione Italiana Ricerca sul cancro (IG21408 grant to CR).

ACKNOWLEDGMENT

We are thankful to Prof. A. Gasco for fruitful discussion.

ABBREVIATIONS

ABC, ATP Binding Cassette; AJ, Adherens Junction; API, Atmospheric Pressure Ionization; BCRP, Breast Cancer Resistance Protein; Caco-2, Caucasian colon adenocarcinoma cell line 2; DAD, Diode Array Detector; EDTA, Ethylenediaminetetraacetic acid; ESI, Electrospray

Ionization; FITC, Fluorescein Isothiocyanate; GI, Gastro-intestinal; HBSS, Hanks' Balanced Salt solution; JAM, Junctional Adhesion Molecule; MDCK, Madin-Darby Canine Kidney; MDR, Multidrug Resistance; MRP, Multidrug Resistance Protein; MTT, 3-(4,5-dimethylthiazol-2-yl)-2,5-diphenyltetrazolium bromide; OATP, Organic Anion Transporter Protein; PBS, Phosphate Buffered Saline; PFA, Paraformaldehyde; P-gp, P-glycoprotein; RP-HPLC, Reversed Phase High Performance Liquid Chromatography; SEM, Standard Error of the Mean; TEER, Trans Epithelial Electrical Resistance; TJ, Tight Junction; TLC, Thin Layer Chromatography; Tris-HCl, Tris(hydroxymethyl)aminomethane hydrochloride; ZO, Zonula Occludens.

REFERENCES

(1) Vancamelbeke, M.; Vermeire, S. The Intestinal Barrier: A Fundamental Role in Health and Disease. *Expert Review of Gastroenterology and Hepatology*. 2017, pp 821–834.

(2) Oshima, T.; Miwa, H. Gastrointestinal Mucosal Barrier Function and Diseases. *Journal of Gastroenterology*. 2016, pp 768–778.

(3) Vermette, D.; Hu, P.; Canarie, M. F.; Funaro, M.; Glover, J.; Pierce, R. W. Tight Junction Structure, Function, and Assessment in the Critically Ill: A Systematic Review. *Intensive Care Med. Exp.* **2018**.

(4) Colabufo, N.; Berardi, F.; Contino, M.; Niso, M.; Perrone, R. ABC Pumps and Their Role in Active Drug Transport. *Curr. Top. Med. Chem.* **2009**, *9* (2), 119–129.

(5) Zhou, S. F. Structure, Function and Regulation of P-Glycoprotein and Its Clinical Relevance in Drug Disposition. *Xenobiotica*. 2008, pp 802–832.

(6) Arana, M. R.; Tocchetti, G. N.; Rigalli, J. P.; Mottino, A. D.; Villanueva, S. S. M. Physiological and Pathophysiological Factors Affecting the Expression and Activity of the Drug Transporter MRP2 in Intestine. Impact on Its Function as Membrane Barrier. *Pharmacol. Res.* **2016**, *109*, 32–44.

(7) Mercado-Lubo, R.; McCormick, B. A. The Interaction of Gut Microbes with Host ABC Transporters. *Gut Microbes*. 2010, pp 301–306.

(8) Cario, E. P-Glycoprotein Multidrug Transporter in Inflammatory Bowel Diseases: More Questions than Answers. *World Journal of Gastroenterology*. 2017, pp 1513–1520.

(9) Krishna, R.; Mayer, L. D. Multidrug Resistance (MDR) in Cancer. *Eur. J. Pharm. Sci.* **2000**, *11*, 265–283.

(10) Salaroglio, I. C.; Abate, C.; Rolando, B.; Battaglia, L.; Gazzano, E.; Colombino, E.; Costamagna, C.; Annovazzi, L.; Mellai, M.; Berardi, F.; et al. Validation of Thiosemicarbazone Compounds as P-Glycoprotein Inhibitors in Human Primary Brain-Blood Barrier and Glioblastoma Stem Cells. *Mol. Pharm.* **2019**, *16* (8), 3361–3373.

(11) Amiri-Kordestani, L.; Basseville, A.; Kurdziel, K.; Fojo, A. T.; Bates, S. E. Targeting MDR in Breast and Lung Cancer: Discriminating Its Potential Importance from the Failure of Drug Resistance Reversal Studies. *Drug Resist. Updat.* **2012**, *15* (0), 50–61.

(12) Colabufo, N. A.; Berardi, F.; Cantore, M.; Perrone, M. G.; Contino, M.; Inglese, C.; Niso, M.; Perrone, R.; Azzariti, A.; Simone, G. M.; et al. Small P-Gp Modulating Molecules: SAR Studies on Tetrahydroisoquinoline Derivatives. *Bioorganic Med. Chem.* **2008**, *16* (1), 362–373.

(13) Colabufo, N. A.; Berardi, F.; Cantore, M.; Perrone, M. G.; Contino, M.; Inglese, C.; Niso, M.; Perrone, R.; Azzariti, A.; Simone, G. M.; et al. 4-Biphenyl and 2-Naphthyl Substituted 6,7-Dimethoxytetrahydroisoquinoline Derivatives as Potent P-Gp Modulators. *Bioorganic Med. Chem.* **2008**, *16* (7), 3732–3743.

(14) Colabufo, N. A.; Berardi, F.; Perrone, M. G.; Cantore, M.; Contino, M.; Inglese, C.; Niso, M.; Perrone, R. Multi-Drug-Resistance-Reverting Agents: 2-Aryloxazole and 2-Arylthiazole Derivatives as Potent BCRP or MRP1 Inhibitors. *ChemMedChem* **2009**, *4* (1), 188–195.

(15) Colabufo, N. A.; Contino, M.; Cantore, M.; Capparelli, E.; Perrone, M. G.; Cassano, G.; Gasparre, G.; Leopoldo, M.; Berardi, F.; Perrone, R. Naphthalenyl Derivatives for Hitting P-Gp/MRP1/BCRP Transporters. *Bioorganic Med. Chem.* **2013**, *21* (5), 1324–1332.

(16) Contino, M.; Zinzi, L.; Cantore, M.; Perrone, M. G.; Leopoldo, M.; Berardi, F.; Perrone, R.; Colabufo, N. A. Activity-Lipophilicity Relationship Studies on P-Gp Ligands Designed as Simplified Tariquidar Bulky Fragments. *Bioorganic Med. Chem. Lett.* **2013**, *23* (13), 3728–3731.

(17) Contino, M.; Zinzi, L.; Perrone, M. G.; Leopoldo, M.; Berardi, F.; Perrone, R.; Colabufo, N. A. Potent and Selective Tariquidar Bioisosters as Potential PET Radiotracers for Imaging P-Gp. *Bioorganic Med. Chem. Lett.* **2013**, *23* (5), 1370–1374.

(18) Nesi, G.; Colabufo, N. A.; Contino, M.; Perrone, M. G.; Digiacomo, M.; Perrone, R.; Lapucci, A.; Macchia, M.; Rapposelli, S. SAR Study on Arylmethyloxyphenyl Scaffold: Looking for a P-Gp Nanomolar Affinity. *Eur. J. Med. Chem.* **2014**, *76*, 558–566.

(19) Capparelli, E.; Zinzi, L.; Cantore, M.; Contino, M.; Perrone, M. G.; Luurtsema, G.; Berardi, F.; Perrone, R.; Colabufo, N. A. SAR Studies on Tetrahydroisoquinoline Derivatives:

The Role of Flexibility and Bioisosterism to Raise Potency and Selectivity toward P-Glycoprotein. *J. Med. Chem.* **2014**, *57* (23), 9983–9994.

(20) Teodori, E.; Dei, S.; Floriddia, E.; Perrone, M. G.; Manetti, D.; Romanelli, M. N.; Contino, M.; Colabufo, N. A. Arylamino Esters As P-Glycoprotein Modulators: SAR Studies to Establish Requirements for Potency and Selectivity. *ChemMedChem* **2015**, *10* (8), 1339–1343.

(21) Capparelli, E.; Contino, M.; Perrone, M. G.; Berardi, F.; Perrone, R.; Leopoldo, M.; Colabufo, N. A. Functionalized Coumarine Fragment to Obtain Fluorescent and Selective P-Glycoprotein Ligands. *Arch. Pharm. (Weinheim).* **2016**, *349* (3), 161–167.

(22) Guglielmo, Stefano Lazzarato, L.; Contino, M.; Perrone, M. G.; Chegaev, K.; Carrieri, A.; Fruttero, R.; Colabufo, N. A.; Gasco, A. Structure-Activity Relationship Studies on Tetrahydroisoquinoline Derivatives: [4'-(6,7-Dimethoxy-3,4-Dihydro-1H-Isoquinolin-2-Ylmethyl)Biphenyl-4-Ol] (MC70) Conjugated through Flexible Alkyl Chains with Furazan Moieties Gives Rise to Potent and Selective. *J. Med. Chem.* **2016**, *59* (14), 6729–6738.

(23) Guglielmo, S.; Contino, M.; Lazzarato, L.; Perrone, M. G.; Blangetti, M.; Fruttero, R.; Colabufo, N. A. A Potent and Selective P-Gp Modulator for Altering Multidrug Resistance Due to Pump Overexpression. *ChemMedChem* **2016**, *11* (4), 374–376.

(24) Contino, M.; Guglielmo, S.; Perrone, M. G.; Giampietro, R.; Rolando, B.; Carrieri, A.; Zaccaria, D.; Chegaev, K.; Borio, V.; Riganti, C.; et al. New Tetrahydroisoquinoline-Based P-Glycoprotein Modulators: Decoration of the Biphenyl Core Gives Selective Ligands. *Medchemcomm* **2018**, *9* (5), 862–869.

(25) Riganti, C.; Contino, M.; Guglielmo, S.; Perrone, M. G.; Salaroglio, I. C.; Milosevic, V.; Giampietro, R.; Leonetti, F.; Rolando, B.; Lazzarato, L.; et al. Design, Biological Evaluation, and Molecular Modeling of Tetrahydroisoquinoline Derivatives: Discovery of A Potent P-Glycoprotein Ligand Overcoming Multidrug Resistance in Cancer Stem Cells. *J. Med. Chem.* **2019**, *62* (2), 974–986.

(26) Dei, S.; Braconi, L.; Trezza, A.; Menicatti, M.; Contino, M.; Coronnello, M.; Chiaramonte, N.; Manetti, D.; Perrone, M. G.; Romanelli, M. N.; et al. Modulation of the Spacer in N,N-Bis(Alkanol)Amine Aryl Ester Heterodimers Led to the Discovery of a Series of Highly Potent P-Glycoprotein-Based Multidrug Resistance (MDR) Modulators. *Eur. J. Med. Chem.* **2019**, *172* (3), 71–94.

(27) Leopoldo, M.; Nardulli, P.; Contino, M.; Leonetti, F.; Luurtsema, G.; Colabufo, N. A. An Updated Patent Review on P-Glycoprotein Inhibitors (2011-2018). *Expert Opin. Ther. Pat.* **2019**, *29* (6), 455–461.

(28) Teodori, E.; Contino, M.; Riganti, C.; Bartolucci, G.; Braconi, L.; Manetti, D.; Romanelli, M. N.; Trezza, A.; Athanasios, A.; Spiga, O.; et al. Design, Synthesis and Biological Evaluation of Stereo- and Regioisomers of Amino Aryl Esters as Multidrug Resistance (MDR) Reversers. *Eur. J. Med. Chem.* **2019**, *182*, 111655.

(29) Ferraretto, A.; Bottani, M.; De Luca, P.; Cornaghi, L.; Arnaboldi, F.; Maggioni, M.; Fiorilli, A. Morphofunctional Properties of a Differentiated Caco2/HT-29 Co-Culture as an in Vitro Model of Human Intestinal Epithelium. *Biosci. Rep.* **2018**, *38* (2), BSR20171497 1-16.

(30) Gupta, V.; Doshi, N.; Mitragotri, S. Permeation of Insulin, Calcitonin and Exenatide across Caco-2 Monolayers: Measurement Using a Rapid, 3-Day System. *PLoS One* **2013**, *8* (2), e57136 1-9.

(31) Kopecka, J.; Salzano, G.; Campia, I.; Lusa, S.; Ghigo, D.; De Rosa, G.; Riganti, C. Insights in the Chemical Components of Liposomes Responsible for P-Glycoprotein Inhibition. *Nanomedicine Nanotechnology, Biol. Med.* **2014**, *10* (1), 77–87.

(32) Guarnieri, D.; Sánchez-Moreno, P.; Del Rio Castillo, A. E.; Bonaccorso, F.; Gatto, F.; Bardi, G.; Martín, C.; Vázquez, E.; Catelani, T.; Sabella, S.; et al. Graphene Biotransformation: Biotransformation and Biological Interaction of Graphene and Graphene Oxide during Simulated Oral Ingestion (Small 24/2018). *Small* **2018**, *14* (24), e1800227.

(33) Riganti, C.; Kopecka, J.; Barak, S.; Rubinstein, M. The Role of C/EBP-β LIP in Multidrug Resistance. *J. Natl. Cancer Inst.* **2015**, *107* (5), djv046.

(34) Hessel, S.; Gottschalk, C.; Schumann, D.; These, A.; Preiss-Weigert, A.; Lampen, A. Structure-Activity Relationship in the Passage of Different Pyrrolizidine Alkaloids through the Gastrointestinal Barrier: ABCB1 Excretes Heliotrine and Echimidine. *Mol. Nutr. Food Res.* **2014**, *58* (5), 995–1004.

(35) Liang, C.; Zhao, J.; Lu, J.; Zhang, Y.; Ma, X.; Shang, X.; Li, Y.; Ma, X.; Liu, M.; Wang, X. Development and Characterization of MDR1 (Mdr1a/b) CRISPR/Cas9 Knockout Rat Model. *Drug Metab. Dispos.* **2019**, *47* (2), 71–79.

(36) Mori, N.; Yokooji, T.; Murakami, T. Fate of Quinidine, a P-Glycoprotein Substrate, in the Gastrointestinal Tract after Oral Administration in Rats. *Pharmazie* **2008**, *63* (3), 241–244.

(37) Rautio, J.; Humphreys, J. E.; Webster, L. O.; Balakrishnan, A.; Keogh, J. P.; Kunta, J. R.; Serabjit-Singh, C. J.; Polli, J. W. In Vitro P-Glycoprotein Inhibition Assays for Assessment of Clinical Drug Interaction Potential of New Drug Candidates: A Recommendation for Probe Substrates. *Drug Metab. Dispos.* **2006**, *34* (5), 786–792.

(38) Raish, M.; Ahmad, A.; Ansari, M. A.; Alkharfy, K. M.; Ahad, A.; Al-Jenoobi, F. I.; Al-Mohizea, A. M.; Khan, A.; Ali, N. Effects of Sinapic Acid on Hepatic Cytochrome P450 3A2, 2C11, and Intestinal P-Glycoprotein on the Pharmacokinetics of Oral Carbamazepine in Rats: Potential Food/Herb-Drug Interaction. *Epilepsy Res.* **2019**, *153*, 14–18.

(39) Clarke, G.; O'Mahony, S. M.; Cryan, J. F.; Dinan, T. G. Verapamil in Treatment Resistant Depression: A Role for the P-Glycoprotein Transporter? *Hum. Psychopharmacol.* **2009**, *24* (3), 217–223.

(40) Shao, X.; Carpenter, G. M.; Desmond, T. J.; Sherman, P.; Quesada, C. A.; Fawaz, M.; Brooks, A. F.; Kilbourn, M. R.; Albin, R. L.; Frey, K. A.; et al. Evaluation of [11C] N-Methyl Lansoprazole as a Radiopharmaceutical for PET Imaging of Tau Neurofibrillary Tangles. *ACS Med. Chem. Lett.* **2012**, *3* (11), 936–941.

(41) Kageyama, M.; Namiki, H.; Fukushima, H.; Terasaka, S.; Togawa, T.; Tanaka, A.; Ito, Y.; Shibata, N.; Takada, K. Effect of Chronic Administration of Ritonavir on Function of Cytochrome P450 3A and P-Glycoprotein in Rats. *Biol. Pharm. Bull.* **2005**, *28* (1), 130–137.

(42) Mariappan, T. T.; Singh, S. Evidence of Efflux-Mediated and Saturable Absorption of Rifampicin in Rat Intestine Using the Ligated Loop and Everted Gut Sac Techniques. *Mol. Pharm.* **2004**, *1* (5), 363–367.

(43) Hamilton, K. O.; Yazdanian, M. A.; Audus, K. L. Modulation of P-Glycoprotein Activity in Calu-3 Cells Using Steroids and β-Ligands. *Int. J. Pharm.* **2001**, *228* (1–2), 171–179.

(44) Singh, S. P.; Wahajuddin; Raju, K. S. R.; Ali, M. M.; Kohli, K.; Jain, G. K. Reduced Bioavailability of Tamoxifen and Its Metabolite 4-Hydroxytamoxifen after Oral Administration with Biochanin A (an Isoflavone) in Rats. *Phyther. Res.* **2012**, *26* (2), 303–307.

(45) Callaghan, R.; Luk, F.; Bebawy, M. Inhibition of the Multidrug Resistance P-Glycoprotein: Time for a Change of Strategy? *Drug Metab. Dispos.* **2014**, *42* (4), 623–631.

(46) Petryszyn, P. W.; Wiela-Hojeńska, A. The Importance of the Polymorphisms of the ABCB1 Gene in Disease Susceptibility, Behavior and Response to Treatment in Inflammatory Bowel Disease: A Literature Review. *Advances in clinical and experimental medicine : official organ Wroclaw Medical University*. 2018, pp 1459–1463.

For Table of Contents Only